February 19, 2016

Gregory J. Frost
Chemical Sciences Division, Earth System Research Laboratory
National Oceanic and Atmospheric Administration
325 Broadway, Mail Stop R/CSD4
Boulder, CO 80305-3328

Dear editor,

Concerning our study on $NO_x$ lifetimes and emissions estimated by satellite observations (acp-2015-633), we have now submitted revisions of the manuscript and supplement.

We have considered all the comments and suggestions from the reviewers carefully and modified the manuscript accordingly. The changes mainly affect the discussion and treatment of uncertainties (section 2.3), in particular related to the involved ECMWF wind fields. In addition, the respective section in the supplement (sect. 3) was largely extended, including the discussion of possible effects of systematic spatio-temporal patterns (e.g., diurnal cycles of $NO_x$ lifetimes) or the assumptions of a constant $NO/NO_2$ ratio and the treatment of the chemical decay of $NO_2$ as a simple first-order loss.

We have also made substantial changes to the supplement, however, In addition to the extended discussion of uncertainties (section 3), new sections about the potential impact of interfering sources (section 4) and possible application of the method for $SO_2$ (section 5) have been added.

While the basic method and thus the resulting lifetime and emission estimates have not been changed, the estimated uncertainties have been slightly modified by
a) adjusting the estimated uncertainty due to wind fields from 20% to 30%, and
b) using the standard mean error (instead of the standard deviation) for the estimated uncertainty of lifetimes from different wind directions.
Due to the latter choice, the final uncertainties slightly decrease.

Looking forward to hearing from you.
Sincerely yours,

Qiang Zhang

Anonymous Referee #1

*This manuscript, titled "$NO_x$ lifetimes and emissions of hotspots in polluted background estimated by satellite observations" by Liu et al. is an interesting addition to continuing line of research, making use of an innovative approach to make lifetime and emission estimates for sources in strong source regions. The paper is clearly written, except for a few noted word- or phase choices, and is well-suited for publication to ACP. However, there are several concerns that should be addressed or considered before being accepted for publication.*

**Response:** We thank Referee #1 for the encouraging comments. All comments and suggestions have been considered carefully and well addressed.

*Major comments:*

*1. Wind effect: Please make note on the possible importance of comments below, or confirm or deny.*

**Response:** We agree that the impact of wind uncertainties on the total estimated emission uncertainty is an important issue which has to be discussed more comprehensively in the paper. We thus extended the paper in this respect by (a) reviewing the error estimate performed by Beirle et al. (2011) within Sect.2.2.1, (b) discussing the effects of uncertainty in wind speeds and directions on estimated lifetimes and emissions within the main paper, and (c) extending the discussion of sophisticated uncertainties related to winds (and other effects) in the supplement. In addition, we have adjusted the final uncertainty estimate associated with wind fields from 20% to 30%.

*The authors need to make it clear in the main text that uncertainty in wind speeds biases lifetime measurements low and thus biases emissions high, as shown by de Foy et al. The authors make this point clearly in the supplementary information but can make it more strongly in the main section.*

**Response:** We agree that the discussion about wind comparison is very important (as stated in the last response), but the effect of the difference between ECMWF and sonde projected wind speeds on estimated lifetimes and emissions is not as drastic as it sounds (in fact, their mean unprojected winds agree within 10%), and can be understood by the sorting procedure, which is explained in detail in the supplement (see also the response for comment 3). We have added one sentence to point out this in Sect.2.6 of the revised manuscript as well.

*2. Evaluation of ERA with sonde data should be moved to supplementary information. It is not the main point of the paper.*

**Response:** We agree that the evaluation of ERA with sonde data is not the main point of the paper, but it clearly shows that mountainous wind data is highly uncertain, which we consider as an important aspect for the general applicability of our approach, and thus should be part of the main paper.

*3. However, the main findings of the wind analysis should be clearly summarized, particularly the finding that wind speeds in ERA are biased low by more than ~20% at all sites, and by ~40% at mountainous sites (Table S3 percent bias and $r^2$). I would also expect that this bias in wind speed should be independent of the bias caused by uncertainty in wind direction (see above comment).*

**Response:** We summarize main findings of the wind analysis in Sect.3 of the supplement, as follows:

"We carried out a comparison of wind information between ECMWF and sounding measurements (Table S3). Here we focus on the comparison of the quantity used for the lifetime estimate, i.e. the projected wind components for each wind direction sector. We firstly sorted ECMWF wind fields for the years 2005–2013 into 8 wind direction sectors and classified the simultaneous sonde data into the same wind direction sector, and then calculate the mean of the projected wind speeds from both datasets to compare. While *total* wind speeds from ECMWF and sonde measurements agree quite well (~5% on average for wind speeds>2 m/s), the *projected* wind components are systematically higher for ECMWF. This can be expected, as ECMWF wind fields are the basis for the wind direction classification. If, for instance, the true wind would be 5 m $s^{-1}$ from north, but the model wind is 5 m $s^{-1}$ from east, the case is classified as easterly, while the actual easterly wind component is 0. That is, deviations of the wind direction (even if 0 on average) cause a systematic bias due to this projection procedure. Thus, the deviation of the projected wind speeds reflects uncertainties of the sorting procedure caused by deviations of the wind direction, and allows for an estimate of the overall uncertainty due to wind fields. The deviations for non-mountainous sites are, on average, acceptable (26%). Note also that de Foy et al. (2015) report on ERA-Interim winds yielding a better lifetime estimate compared to the North American Regional Reanalysis project (NARR). For mountainous sites, however, significantly higher deviations are found (37% on average) due to insufficient spatial resolution of ECMWF (see also Sect. 2.6 of the manuscript). **"**

*4. There is a strong diurnal increase in wind speed over land from morning to afternoon (e.g,. Dai et al,. 1999; 10.1029/1999JD900927). I expect that this will also bias inferred lifetimes low.*

*Many large sources are coastal. Sharp temperature gradients will also induce local circulation biases that may affect wind analysis in a similar manner as suggested by comments above.*

**Response:** We have discussed this in Sect.3 of the supplement, as follows:

"Wind fields often reveal systematic spatio-temporal patterns, such as diurnal cycles or land-sea transitions, which could have systematic effects on our results. As the underlying physical processes are included in the models, these effects should, in first order, be accounted for by ECMWF. However, the spatial resolution might be too coarse to capture these effects completely.

Beirle et al. (2011) varied the time of the wind data used for the fit and found changes below 10%. In addition, from the comparison with sonde data, we see no indication that ECMWF data are particularly biased for coastal cities (Miami, Xiamen). We thus

consider the uncertainties caused by diurnal cycles of wind speeds or land-sea transitions to be covered by the estimated overall uncertainty related to wind fields. Overall, we estimate the uncertainties associated with the wind data as 30% for non-mountainous sites."

*5. The authors should briefly discuss their results in the context of de Foy et al who simulated a tracer with a well-behaved lifetime and realistic wind patterns.*
**Response:** Thanks. We have added the discussion in the introduction of the revised manuscript, as follows:
"de Foy et al. (2014) further analyzed the performance of the method using model simulations with fixed a-priori lifetimes and realistic wind data, which proved that the fitted results were accurate in general and showed best performance for strong wind cases."

*6. Chemical effects: We do not expect the authors to fully account for all effects, but rather hope they clarify their potential impact on the results in the text.*
*L194 24 "we could not unambiguously relate the variability of $NO_x$ to a driving parameter like surface elevations, mean wind or latitude." What about VOC? Could any links be made? It would seem that there should be some systematic dependence, especially with latitude. $SO_2$ has a much longer lifetime, does it have any different spatial pattern? Sources of $SO_2$ in China should be large enough to perform the analysis. If so, does that suggest that mixing processes and instrumental resolution are putting an upper limit on inferred lifetimes?*
*There are very large gradients in VOC in the regions of interest. We would expect some influence of VOC on the lifetime (reduces OH sink, but increases RO2 sinks).*
**Response:** We thank the reviewer for these suggestions.
VOC: In order to investigate a potential link between VOCs and the estimated $NO_x$ lifetimes, we used the tropospheric $H_2CO$ columns as provided by BIRA (De Smedt et al., 2015) from OMI observations. We averaged the $H_2CO$ columns for the ozone season during 2005−2013, and explore their relationship with $NO_x$ lifetime. We observed systematic spatial patterns for the $H_2CO$ columns, e.g., the concentration of $H_2CO$ is higher in the eastern US than the western US, which is similar to the spatial distribution of $NO_x$ lifetime. However, the overall correlation between $H_2CO$ TVCDs and $NO_x$ lifetime is rather low ($r^2 = 0.13$). Thus, we see no indication that VOCs are the main driver for the spatial variability of $NO_x$ lifetime. We have discussed this in Sect. 3.1 of the revised manuscript.
$SO_2$: We have added the text to the end of Sect. 3.2, as follows:
"Satellite observations also enable the study of spatial and temporal distributions of $SO_2$ emissions (e.g., Fioletov et al. (2011)) and even to obtain estimates of $SO_2$ lifetimes and emissions under special circumstances (e.g., Beirle et al. (2014)). However, if the method developed in this study would be applied to $SO_2$ directly, higher uncertainties have to be expected due to the longer lifetime of $SO_2$ (see Sect. 5 of the supplement for a detailed discussion)."
We have also added a new section (Sect.5) to the supplement, as follows:

“5. Potential applications for $SO_2$

We have presented a method for the estimation of $NO_x$ lifetimes and emissions from space for strong sources on top of a generally polluted background.
Satellite observations of $SO_2$ have been used before for top-down estimates of emissions (e.g., Fioletov et al., 2011) and even to obtain estimates of $SO_2$ lifetimes under special circumstances. Beirle et al. (2014) analyzed downwind plume evolution of $SO_2$ from the Kilauea volcano on Hawaii and estimated the respective $SO_2$ lifetime and emissions by a method similar to that proposed in Beirle et al. (2011) for $NO_2$. In this special case, however, wind conditions were pretty stable, and only one main wind direction had to be considered, without any sorting, due to the prevailing trade winds.
For multiple sources in polluted background and variable wind conditions, however, the situation for $SO_2$ is much more complex than for $NO_2$: The $NO_2$ observations are sorted according to the wind direction at the time of the measurement, while the “history” (i.e. the potential impact of $NO_x$ emissions from the previous day, transported under possibly different wind conditions) is not considered. While this is appropriate for $NO_2$ due to the lifetime of a few hours, this is fundamentally different for $SO_2$ with longer lifetimes, which causes considerably higher uncertainties due to changes of wind directions. In addition, also the across-wind integration (needed to compensate for spatial dilution) as well as the fit would have to be performed on larger intervals for longer lifetimes, such that nearby sources cannot be separated from each other anymore and the quantification of $SO_2$ emissions from an individual source would be more difficult.
Thus, it might be worth testing a similar method for $SO_2$, but one has to be aware of the potential drawbacks, and we expect a higher uncertainty of resulting emissions as a consequence of the generally longer lifetime of $SO_2$.”

*7. The authors suggest that any uncertainty in the $NO_2$:NO ratio will only affect emission estimates. However, there are two ways in which this can interfere with inference of the lifetime. In cities where incoming $O_3$ is very low (e.g., as low as 20 ppb. Houston,Gulf air), $O_3$ production in the plume up to 100 ppb. will have a five fold effect on the $NO_2$:NO ratio downwind (1:1 vs 5:1 -> a 60% increase in $NO_2$:NOx), an apparent increase in $NO_2$ where the true $NO_x$ lifetime should decrease (more $NO_2$ available to react with OH as well as more $RO_2$ and OH from $O_3$ photolysis). A second effect is related to mixing and the NO:$NO_2$ ratio. The lifetime inferred by this study is very similar to values for the timescales of dilution with the free troposphere used in field studies (Zaveri et al., 2002 - doi:10.1029/2002JD003144 ; Wang et al., 2006 -0.1029/2006GL027689 ). In the FT, winds are often faster and from a different direction than at the surface and the NO:$NO_2$ ratio favors NO due to much faster photolysis(e.g., Dickerson et al., 1997 10.1126/science.278.5339.827) and lower number densities (i.e., J[NO2]/k[NO][O3]). These effects are in addition to latitudinal and altitude impacts which are nominally mentioned in the text.*
**Response:** Concerning the first point, we generally agree that changes of the

$NO_2/NO_x$ ratio could influence the $NO_x$ lifetime, in particular if the difference in $O_3$ concentrations between upwind and downwind plumes is significant.
We have discussed this in Sect.3 of the supplement, as follows:
"However, the $NO/NO_2$ ratio of course might differ locally, in particular when the difference in $O_3$ concentrations between upwind and downwind plumes is significant. But the influence is not dramatic on the scales of the OMI footprint (at least 13 km×24 km). In addition, the influence has been included in the overall uncertainty estimates by averaging the fit results for different wind direction sectors that usually represent different levels of incoming $O_3$. We consider the applied correction (with an assumed uncertainty of 10%), to be adequately represented by the CTM, reflecting the mean conditions over spatial scales of ~100−200 km."

With respect to vertical profiles, we have checked the impact of different altitudes used for the extraction of horizontal wind fields (compare also Beirle et al., 2011), and found the dependencies to be low (~10%) and covered by the overall uncertainty due to wind fields. However, we could not find the statement that fresh $NO_x$ emissions mix with the free troposphere within a few hours in the cited references: (Zaveri et al.(2002) explained the relationship between ozone production and $NO_x$ by model simulations, but the set of model seems to only consider the vertical mixing within the PBL (Sect. 4.1). The work in Wang et al. (2006) seems not to deal with the free troposphere as well.)

*8. Retrieval effects: $NO_2$ products using coarse resolution inputs for converting slant columns to vertical columns have a very different urban to regional gradients than those using higher resolution inputs (e.g., Russell et al., 2011 - doi:10.5194/acp-11-8543-2011). It is unclear which is best for this purpose, as one would bias the background high whereas the other would bias urban plumes extending in to the background low, but this difference is likely worth noting.*
**Response:** Thanks. We have added the discussion in the Sect.3 of the supplementary information of the revised manuscript, as follows:
"Though the recent update of the DOMINO algorithm (Boersma et al., 2011) has improved some issues related to the spatial resolution of external databases, retrievals are still based on relatively coarsely resolved terrain height, ground albedo, and a-priori $NO_2$ vertical profile shape, probably causing low-biased VCDs over strong emission sources (e.g., Russell et al., 2011). These effects are, however, covered by the assumed uncertainty of TVCDs of 30%."

*9. Miscellaneous: The seasonal patterns of inferred $NO_x$ lifetime and emissions in Figure S4 indicate that there is far more uncertainty in this method than alluded to in the text. The method infers large seasonal variations of emissions (log scale) and relatively small seasonal variability of lifetime (linear scale). Most would expect the opposite pattern. Please make this result more clear in the text.*
**Response:** The seasonal lifetimes reveal higher uncertainties due to the smaller number of available satellite observations and thus reduced number of wind direction

sectors that yielding a valid fit, compared to the ozone season. The uncertainty is sometimes too large to get reasonable seasonal patterns for a specific location. On top of that, the emission estimate is affected by poorer statistics, in particular in case of spatial gaps, probably causing the large seasonal fluctuations found for some sites. We have clarified this in the Sect. 3.1 of the revised manuscript, as follows:
"The seasonal lifetimes reveal higher uncertainties due to a smaller number of available satellite observations compared to the ozone season and thus reduced number of wind direction sectors that yielding a valid fit. The uncertainty is sometimes too large to get reasonable seasonal patterns for a specific location. But still a systematic seasonal variability can be observed for most non-mountainous cases: mean lifetimes are found to be shorter in summer (3.2 hours) compared to spring (4.2 hours) and autumn (4.5 hours), as expected.
For some locations, the resulting emissions vary considerably over season, which again can be attributed to the poor statistics; in particular spatial gaps cause high uncertainties of the determined total $NO_2$ mass based on Eq. (5)."

*10. For Table S2 Please include more fit statistics for the summertime analysis, including number of fits that meet the criteria out of the 8 directions, and add the +/- 1-sigma lifetime inferred from different directions.*
**Response:** Thanks. We have added it in Table S2 of the revised manuscript

Specific comments:
*11. Title: Consider different word use than "hotspots" in title and throughout.*
**Response:** We have replaced "hotspots" by "Cities and power plants" in title and throughout the paper.

*12. 180 L13-14: The last sentence in the abstract is confusing and should be clarified. In regards to the finding, can you address this at a larger scale by using the average lifetime from valid analyses over a region (e.g, E China or NE China)? Is the result the same?*
**Response:** The different performance between regional inventory MEIC and global inventory EDGAR could not be attributed to the difference in the total budget as the comments concerned, because the deviation in national total $NO_x$ emissions is far less (20.7 and 24.9 Tg-NO2 for year 2008 in EDGAR and MEIC respectively). In addition, the extant inverse estimate at regional level has suggested that top-down national budget is close to the bottom-up emission estimate for East China (Lin et al., 2010). We have revised the last sentence in the abstract in the revised manuscript as follows:
"Regional inventory shows better agreement with top-down estimates for Chinese cities compared to global inventory, most likely due to different downscaling approaches adopted in the two inventories."

*13. 183 Paragraph 1: any impact of new spectral fit? (van Geffen et al., 2015 -doi:10.5194/amt-8-1685-2015)*
**Response:** We are aware of the recent improvements of the spectral analysis for OMI

and add the discussion about these references to the Sect.3 of the supplement, as follows:
"Recently, an overall bias of the OMI $NO_2$ column density has been reported, which turns out to be related to an imperfect spectral analysis and could be removed by improved spectral fitting procedures (van Geffen et al., 2015; Marchenkov et al., 2015). Unfortunately, the updated datasets are not available yet.
However, as an overall bias in total columns is mostly removed by the stratospheric correction procedures, we do not expect a large effect on the tropospheric $NO_2$ column densities over polluted sites, and thus no impact on our emission estimates."

*14. 183 L5 - Please, if available, cite and state numbers of any source that quantifies difference of this version of DOMINO with other products.*
**Response:** Besides the DOMINO v2 $NO_2$ product, also NASA provides an $NO_2$ "standard product" (Bucsela et al., 2013). Both products differ in the retrieval details, in particular in the stratospheric correction and in the a-priori used for the calculation of AMFs (in particular the a-priori $NO_2$ profiles). Overall, both products show a good quantitative agreement (see Fig. 9 in Bucsela et al., 2013). Note also that any additive offset between different products (as caused by different stratospheric corrections) would have no effects on our estimated emissions due to the fitted background in Eq.(5). We have clarified this in Sect.3 of the supplement, as follows:
"The retrievals of $NO_2$ TVCDs performed by KNMI (used in this study) and NASA (OMI "Standard Product") are based on the same spectral analysis, but differ in the separation of stratospheric and tropospheric columns and AMF calculations (Bucsela et al., 2013; Boersma et al., 2011; Boersma et al., 2007; Dirksen et al., 2011), which resulted in some significant differences in their early released products (Lamsal et al., 2010; Platt and Stutz, 2008). With the development of $NO_2$ retrieval algorithms, however, the two products are increasingly converging (Bucsela et al., 2013; Boersma et al., 2011)."

*15. 186 L4: Please list instead of $r^2$ the range of inferred lifetimes and other important parameters. The model may be over-determined .*
**Response:** Thanks. We listed both the range of inferred lifetimes and $R^2$ in the revised manuscript.

*16. 186 Footnote: Does this mean that calm winds are only 2-3% of faster winds?*
**Response:** Yes, the projected wind speed under calm wind and windy conditions is 0.1 and 17.4 km/h on average respectively for investigated sources (for calm, slightly positive and negative projected winds almost cancel out).

*17. 189 - see major comment on $NO_2$:$NO_x$ - a few sentences or a paragraph here should be sufficient.*
**Response:** Please see the response for comment 7.

*18. 191 L8-27 - This paragraph was a bit confusing. It was unclear to me whether the*

*large decreases in the US or large increases in China would effect results by only using 2005-2008. Also, the decrease that is reported seems smaller than reported elsewhere. Does this agree with the rate of decrease observed elsewhere?*

**Response:** In theory, any large changes in $NO_x$ emissions after 2008 would affect results when comparing top-down estimates with bottom-up ones for the years 2005–2008. However, the effect is of minor importance for China. The emission changes in China is not linear after the year 2008: $NO_x$ emissions rebounded after the economic crisis around 2008 and declined again around 2012 associated with emission control regulations. Based on MEIC inventory, the average $NO_x$ emission for investigated Chinese cities for the years 2005–2008 is only 3% less than that for the years 2005–2012. Thus, we only emphasized the effect for the US in the main text.

The decline in $NO_2$ TVCDs over the US observed in this study is comparable with other studies. We observed a decline in $NO_2$ TVCDs from the period of 2005–2008 to the period of 2009–2013 with an average total reduction of 14 ± 9% for investigated US cities. Russell et al. (2012) reported consistent decreases of $NO_2$ TVCDs in cities across the US, with an average total reduction of 32 ± 7 % during 2005–2011. The two decrease rates are comparable.

*19. 192 I think that there should be some justification as to why European sources were not analyzed.*

**Response:** For this study, we choose large sources across China and the US as the pre-selected candidates, of which the good-quality and countrywide consistent bottom-up emission information, particularly for power plants, is available. Further investigation on sources located in other regions, in particular, Europe, will be performed in the near future, with collating the corresponding bottom-up emission inventories. We have clarified this in the Sect.4 of the revised manuscript.

*20. L198 22 - see major comments on wind effects. Please clarify here that the wind speeds are biased high by ~20% and that any additional uncertainty in direction, and potentially diurnal oscillations (i.e., sea breeze, mountain breeze), will lead to biased lifetimes.*

**Response:** Please see the response for comment 3.

*21. L198 25 - Where do these numbers come from? There are definitely conditions where the choice of $NO_2$:$NO_x$ ratio used here is off by more than 10%. Please add reference and value for analysis of different products / validation papers.*

**Response:** The concrete number of 1.3 used for scaling up the $NO_2$ to $NO_x$ is based on the typical assumptions made in the section 6.5.1 of Seinfeld and Pandis (2006) for "typical urban conditions and noontime sun". Note that conditions are quite consistent in this study due to the overpass time of OMI close to noon, the selection of cloud-free observations, the focus on the ozone season, and the focus on polluted regions with generally high tropospheric ozone.

In addition, we have checked the $NO_x/NO_2$ ratio at OMI overpass time within the boundary layer (up to 2 km) with the CTM EMAC (Jöckel et al., 2015) and found

values of 1.28 ± 0.08 for polluted ($NO_x$>1×$10^{15}$ molec $cm^{-2}$) regions in China and the US for the 1st of July 2005, and similar values for all days of the ozone season (on average 1.32 ± 0.06).
While the $NO/NO_2$ ratio of course might differ locally (in particular close to strong sources), we still consider the applied correction (with an assumed uncertainty of 10%), to be adequately represented by the CTM, as it has to represent the mean conditions over spatial scales of ~100−200 km. We have clarified this in the supplementary information of the revised manuscript.

*22. 210 and wind analyses - I would expect that the sonde data have a large influence on the ECMWF re-analysis? I would expect that the comparison at the site and sonde time (0 and 12 UTC) would be good but that might not extend to other locations and times.*
**Response:** The sonde data are indeed incorporated in ECMWE assimilation, but still they are not expected to be the same, as multiple input data are used, and model values are not simply overwritten, but only regulated.
Thus, the deviation between the resulting assimilated ECMWF wind fields and individual sonde measurements can still be significant, in particular in mountainous regions, like shown in Table S3.

*23. 214 - See major comment - If lifetime from all individual sources is averaged in some way and emissions are inverted by mass balance, is there still a large EDGAR underestimate?*
**Response:** The underestimation of EDGAR inventory is less significant at regional scale than urban scale when comparing with top-down estimates using an averaged lifetime or MEIC inventory. As stated in the response for comment 12, the underestimation could not be attributed to the total budget, as the national total $NO_x$ emissions of different inventories are comparable, but is most likely due to different downscaling approaches.

*24. Sup 9 - see major comment. Please make the results of Table S3 much more clear in the text. "Percent change" heading should be "percent difference" and please include (+) or (-) to indicate that all are biased in the same way. Also, I assume that r2 is wind speed. Is there some way to indicate agreement of direction, or u and v components?*
**Response:** Thanks for the suggestions. We have revised the heading and the sign in the revised manuscript. $r^2$ does not refer only to the wind speed, it considers the wind direction. We firstly sorted ECMWF wind fields for the years 2005–2013 into 8 wind direction sectors and classified the simultaneous sonde data into the same wind direction sector, and then calculate the mean of the projected wind speeds from both datasets to calculate $r^2$. We have added a note to clarify this in the table.

*Technical comments:*
*25. 181 L10: "Emissions . . . "sentence should be re-phrased.*

**Response:** Thanks. We have re-phrased the sentence as follows:
"Emissions at city level are often downscaled from regional emission estimates, based on surrogates (e.g. population density and industrial productivity), which however often just roughly reflects the magnitude and spatial distribution of urban emissions."

*26. 181 L22: ". . .allow. . ." consider re-wording.*
**Response:** Thanks. We have re-phrased the sentence as follows:
"The satellite $NO_2$ measurements have been applied to quantify $NO_x$ emissions."

*27. 182 L4 "hotspots" re-word*
**Response:** We have done it (please see the response for comment 11).

*28. 183 L10 "by" different word choice*
**Response:** We have replaced "by" by "from". We would welcome proposals for a better formulation from the reviewer (or the ACP language editor) if needed.

*29. 184 L3: More descriptive section heading "Outflow model'?*
**Response:** Thanks. We have revised the label as "$NO_2$ outflow models and lifetime/emission fits" in the text.

*30. 184 L8 "recap" -> "summarize"*
**Response:** Thanks. We have re-phrased the word in the revised manuscript.

*31. 184 L16. This source is actually reasonably isolated relative to the others. Please identify Harbin on Figure 5.*
**Response:** Thanks. We have identified Harbin on Fig.5 in the revised manuscript.

*32. 184 L1 New label? "Isolated point source outflow model: Lifetime and ENOx"*
**Response:** Thanks. We have revised the label as "Isolated point source outflow model: Lifetime and Emissions" in the text.

*33. 185 L1 New label? "Mixed source outflow model: Lifetime"*
**Response:** Thanks. We have revised the label in the text.

*34. 186 L12 New label? "Mixed source outflow model: Emissions"*
**Response:** Thanks. We have revised the label in the text.

*35. 186 L9 What is the typical number of fits that meet the criteria of the 8 possible?*
**Response:** The number of fits that meet the criteria is 4 on average. We have added this in Sect.2.5 of the revised manuscript.

*36. 192 L9 - It seems like a global database of urban areas or population density would be a better classification for future reference.*
**Response:** The relationship between urban emissions and socio-economic parameters

is complex. For instance, a city with low population density does not necessarily correspond to a small amount of emissions if it has strong industrial activity. However, we do not deny that a global database of urban areas or population density would help to identify the candidates. We would like to explore which indicator is better in a future study.

*37. 211 - As mentioned elsewhere. Please label and emphasize Harbin. If possible label all locations.*
**Response:** Thanks. We have labelled all locations on Fig.5 in the revised manuscript.

*38. Supp 5 L5 direction -> direct*
**Response:** Thanks. We have revised the sentence as follows:
"The accuracy of wind fields affects our analysis twofold, by sorting the NO2 TVCDs according to wind directions as well as by transferring the fitted e-folding distance into a lifetime."

## Reference


Beirle, S., Boersma, K. F., Platt, U., Lawrence, M. G., and Wagner, T.: Megacity emissions and lifetimes of nitrogen oxides probed from space, Science, 333, 1737–1739, 2011.

Beirle, S., Hörmann, C., Penning de Vries, M., Dörner, S., Kern, C., and Wagner, T.: Estimating the volcanic emission rate and atmospheric lifetime of $SO_2$ from space: a case study for Kīlauea volcano, Hawai'i, Atmos. Chem. Phys., 14, 8309–8322, 10.5194/acp-14-8309-2014, 2014.

Boersma, K. F., Eskes, H. J., Veefkind, J. P., Brinksma, E. J., van der A, R. J., Sneep, M., van den Oord, G. H. J., Levelt, P. F., Stammes, P., Gleason, J. F., and Bucsela, E. J.: Near-real time retrieval of tropospheric $NO_2$ from OMI, Atmos. Chem. Phys., 7, 2103–2118, 10.5194/acp-7-2103-2007, 2007.

Boersma, K. F., Eskes, H. J., Dirksen, R. J., van der A, R. J., Veefkind, J. P., Stammes, P., Huijnen, V., Kleipool, Q. L., Sneep, M., Claas, J., Leitão, J., Richter, A., Zhou, Y., and Brunner, D.: An improved tropospheric $NO_2$ column retrieval algorithm for the Ozone Monitoring Instrument, Atmos. Meas. Tech., 4, 1905–1928, doi:10.5194/amt-4-1905-2011, 2011.

Bucsela, E. J., Krotkov, N. A., Celarier, E. A., Lamsal, L. N., Swartz, W. H., Bhartia, P. K., Boersma, K. F., Veefkind, J. P., Gleason, J. F., and Pickering, K. E.: A new stratospheric and tropospheric $NO_2$ retrieval algorithm for nadir-viewing satellite instruments: applications to OMI, Atmos. Meas. Tech., 6, 2607–2626, doi:10.5194/amt-6-2607-2013, 2013.

de Foy, B., Wilkins, J. L., Lu, Z., Streets, D. G., and Duncan, B. N.: Model evaluation of methods for estimating surface emissions and chemical lifetimes from satellite data, Atmos. Environ., 98, 66–77, 2014.

de Foy, B., Lu, Z., Streets, D. G., Lamsal, L. N., and Duncan, B. N.: Estimates of power plant $NO_x$ emissions and lifetimes from OMI $NO_2$ satellite retrievals, Atmos. Environ., 116, 1–11, 2015.

De Smedt, I., Stavrakou, T., Hendrick, F., Danckaert, T., Vlemmix, T., Pinardi, G., Theys, N., Lerot, C., Gielen, C., Vigouroux, C., Hermans, C., Fayt, C., Veefkind, P., Müller, J. F., and Van Roozendael, M.: Diurnal, seasonal and long-term variations of global formaldehyde columns inferred from combined OMI and GOME-2 observations, Atmos. Chem. Phys., 15, 12519–12545, doi: 10.5194/acp-15-12519-2015, 2015.

Dirksen, R. J., Boersma, K. F., Eskes, H. J., Ionov, D. V., Bucsela, E. J., Levelt, P. F., and Kelder, H. M.: Evaluation of stratospheric $NO_2$ retrieved from the Ozone Monitoring Instrument: Intercomparison, diurnal cycle, and trending, Journal of Geophysical Research: Atmospheres, 116, D08305, doi: 10.1029/2010JD014943, 2011.

Fioletov, V. E., McLinden, C. A., Krotkov, N., Moran, M. D., and Yang, K.: Estimation of $SO_2$ emissions using OMI retrievals, Geophys. Res. Lett., 38, L21811, doi: 10.1029/2011gl049402, 2011.

Jöckel, P., Tost, H., Pozzer, A., Kunze, M., Kirner, O., Brenninkmeijer, C. A. M., Brinkop, S., Cai, D. S., Dyroff, C., Eckstein, J., Frank, F., Garny, H., Gottschaldt, K. D., Graf, P., Grewe, V., Kerkweg, A., Kern, B., Matthes, S., Mertens, M., Meul, S., Neumaier, M., Nützel, M., Oberländer-Hayn, S., Ruhnke, R., Runde, T., Sander, R., Scharffe, D., and Zahn, A.: Earth System Chemistry Integrated Modelling (ESCiMo) with the Modular Earth Submodel System (MESSy, version 2.51), Geosci. Model Dev. Discuss., 8, 8635–8750, doi: 10.5194/gmdd-8-8635-2015, 2015.

Lamsal, L. N., Martin, R. V., van Donkelaar, A., Celarier, E. A., Bucsela, E. J., Boersma, K. F., Dirksen, R., Luo, C., and Wang, Y.: Indirect validation of tropospheric nitrogen dioxide retrieved from the OMI satellite instrument: Insight into the seasonal variation of nitrogen oxides at northern midlatitudes, Journal of Geophysical Research: Atmospheres, 115, D05302, doi: 10.1029/2009JD013351, 2010.

Lin, J. T., McElroy, M. B., and Boersma, K. F.: Constraint of anthropogenic $NO_x$ emissions in China from different sectors: a new methodology using multiple satellite retrievals, Atmos. Chem. Phys., 10, 63-78, doi: 10.5194/acp-10-63-2010, 2010.

Marchenko, S., Krotkov, N. A., Lamsal, L. N., Celarier, E. A., Swartz, W. H., and Bucsela, E. J.: Revising the slant column density retrieval of nitrogen dioxide observed by the Ozone Monitoring Instrument, Journal of Geophysical Research: Atmospheres, 120, 5670–5692, doi:10.1002/2014jd022913, 2015.

Platt, U., and Stutz, J.: Differential absorption spectroscopy, 135–174, Berlin and Heidelberg, Germany, Springer, 2008.

Russell, A. R., Perring, A. E., Valin, L. C., Bucsela, E. J., Browne, E. C., Wooldridge, P. J., and Cohen, R. C.: A high spatial resolution retrieval of $NO_2$ column densities from OMI: method and evaluation, Atmos. Chem. Phys., 11, 8543–8554, doi: 10.5194/acp-11-8543-2011, 2011.

Anonymous Referee #2

*General comments*

*The proposed method is an extension of a previous method developed by the same author's for estimating $NO_x$ emission and lifetime from satellite-based observations. It is a very elegant approach, as not dependent on modeling assumptions. In this manuscript the method is extended to sources located in polluted background, while it was presented originally only for megacities with relatively low background pollution. Uncertainties on emission estimates are still very large and this study contributes n reducing these uncertainties. The paper is well written and the methodology appropriate. I recommend publication on ACP after addressing the following specific and technical comments.*

**Response:** We thank Referee #2 for the encouraging comments. We addressed the comments carefully as below.

*Specific comments*

*1) P24182 L9 You could maybe mention the nominal spatial resolution at nadir here.*

**Response:** Thanks. We have mentioned it in the revised manuscript.

*2) P24 L13-14 I think the reference to other works could be improved.*

*You might want to cite a similar methodology for fitting described by: Fioletov, V. E., C. A. McLinden, N. Krotkov, M. D. Moran, and K. Yang (2011), Estimation of $SO_2$ emissions using OMI retrievals, Geophys. Res. Lett., 38, L21811, doi:10.1029/2011GL049402.*

*Or more recently in: Fioletov, V. E., C. A. McLinden, N. Krotkov, and C. Li (2015), Lifetimes and emissions of $SO_2$ from point sources estimated from OMI. Geophys. Res. Lett., 42, 1969–1976. doi: 10.1002/2015GL063148."*

*You could also discuss more in the introduction for example the results (including e.g. the advantages and disadvantages) of the methodologies presented by Valin et al. (2013), Lu et al. (2015) and de Foy et al. (2015). At the moment these papers are just mentioned. What were their main features and results?*

**Response:** We have clarified the main features and results of the above references in the revised manuscript, as follows:

"In a recent study, Beirle et al. (2011) averaged OMI $NO_2$ measurements separately for different wind directions, thereby constructing clear downwind plumes which allow a simultaneous fit of the effective $NO_x$ lifetimes and emissions, without the need of a chemical model. Valin et al. (2013) adopted this approach, but rotated satellite $NO_2$ observations according to wind directions such that all the $NO_2$ columns are aligned in one direction (from upwind to downwind). The rotation procedure accumulated a statistically significant data set to examine the dependence of $NO_x$ lifetime on the wind speed. Following studies e.g. de Foy et al. (2015) and Lu et al. (2015) adopted this plume rotation technique and quantified $NO_x$ emissions from isolated power plants and cities over the US respectively, which showed that the method can gave reliable estimates over multi-annual averages and even provide

estimates of emission trends with reasonable accuracy. de Foy et al. (2014) further analyzed the performance of the method using model simulations with fixed a-priori lifetimes and realistic wind data, which proved that the fitted results were accurate in general and showed best performance for strong wind cases. Alternative approaches based on model functions with multiple dimensions, e.g. a two dimensional Gaussian functions (Fioletov et al., 2011) and a three dimensional function (Fioletov et al., 2015), were also proposed to estimate lifetimes and emissions. “

*Could you also comment on the applicability of your methodology for $SO_2$ polluted sources too somewhere in the manuscript?*

**Response:** We thank the reviewer for this request, which is of course an obvious question. We have added the text to the end of Sect. 3.2, as follows:

“Satellite observations also enable the study of spatial and temporal distributions of $SO_2$ emissions (e.g., Fioletov et al. (2011)) and even to obtain estimates of $SO_2$ lifetimes and emissions under special circumstances (e.g., Beirle et al. (2014)). However, if the method developed in this study would be applied to $SO_2$ directly, higher uncertainties have to be expected due to the longer lifetime of $SO_2$ (see Sect. 5 of the supplement for a detailed discussion).”

We have also added a new section (Sect.5) to the supplement, as follows:

“5. Potential applications for $SO_2$

We have presented a method for the estimation of $NO_x$ lifetimes and emissions from space for strong sources on top of a generally polluted background.

Satellite observations of $SO_2$ have been used before for top-down estimates of emissions (e.g., Fioletov et al., 2011) and even to obtain estimates of $SO_2$ lifetimes under special circumstances. Beirle et al. (2014) analyzed downwind plume evolution of $SO_2$ from the Kilauea volcano on Hawaii and estimated the respective $SO_2$ lifetime and emissions by a method similar to that proposed in Beirle et al. (2011) for $NO_2$. In this special case, however, wind conditions were pretty stable, and only one main wind direction had to be considered, without any sorting, due to the prevailing trade winds.

For multiple sources in polluted background and variable wind conditions, however, the situation for $SO_2$ is much more complex than for $NO_2$: The $NO_2$ observations are sorted according to the wind direction at the time of the measurement, while the “history” (i.e. the potential impact of $NO_x$ emissions from the previous day, transported under possibly different wind conditions) is not considered. While this is appropriate for $NO_2$ due to the lifetime of a few hours, this is fundamentally different for $SO_2$ with longer lifetimes, which causes considerably higher uncertainties due to changes of wind directions. In addition, also the across-wind integration (needed to compensate for spatial dilution) as well as the fit would have to be performed on larger intervals for longer lifetimes, such that nearby sources cannot be separated from each other anymore and the quantification of $SO_2$ emissions from an individual source would be more difficult.

Thus, it might be worth testing a similar method for $SO_2$, but one has to be aware of

the potential drawbacks, and we expect a higher uncertainty of resulting emissions as a consequence of the generally longer lifetime of $SO_2$. ”

*3) P24186 L7-8 You mention here that 8 wind sectors are used for lifetime estimation but later in section 2.2.3a only 4 sectors are considered for Eq. 5 when emissions are estimated. Could you comment on that?*
**Response:** We have clarified this in the sect. 2.2.3 of the revised manuscript, as follows:
“Note that the projections of line densities under calm wind conditions for opposite wind direction sectors, e.g., north and south, are just mirrored. Thus, we combined the projections for opposite wind direction sectors.”

*4) P24190 L15 Because only clear sky pixels are considered you might want to comment also on the eventual bias on emission and lifetime due to for example to specific wind patterns and accelerated photochemistry under clear sky conditions.*
**Response:** We agree that the selection of cloud-free OMI $NO_2$ TVCDs used for fitting lifetimes and emissions does not represent the average level for all days, due to the accelerated photochemistry and different meteorological conditions (e.g. boundary layer height, atmospheric transport) under clear sky conditions. But still the emission estimates are appropriate, as both the $NO_x$ lifetime and total mass derived from the $NO_2$ TVCDs are derived consistently, both of which reflect the values under clear sky conditions. Thus, this effect is of minor importance for this study and is not expected to bias the estimates of $NO_x$ emissions. We have included this aspect in Sect. 3 of the revised supplement.

*5) P24191 L25 and Fig. S3 I think that this kind of methods would be useful to estimate changes in emissions over time. Would it be feasible to estimate the emissions for these two different periods (2005-2008 and 2009-2013) in order to quantify the emission reduction expected in US east-coast? If so, could you provide the results?*
**Response:** We have reprocessed the data for the US according to the reviewer’s comment. Unfortunately, the fit procedure of emissions only works for a very limited number of sources for the period of 2009–2013, due to the lack of observations as a consequence of the row anomaly after 2008. However, the capability of estimating emissions for shorter time periods will be enhanced with future satellite instrument like TROPOMI (Veefkind et al., 2012) featuring higher spatial resolution, and in particular by upcoming geostationary satellite instruments, as stated in the conclusions.

*6) P24200 L16-18 Could you comment more on how the methodology is applicable elsewhere, e.g. in Europe? I suppose there the emission source patterns might be even on smaller scale. In the original paper (Beirle et al. 2011) only 2 European cities, Madrid and Moscow, were included, and Helsinki (plus Saint Petersburg and Stockholm) in a following paper by Ialongo et al. (2014) so I suppose Europe would*

*be one of the main areas to assess the applicability of this new method. Could you comment on that?*

**Response:** For this study, we choose large sources across China and the US as the pre-selected candidates, of which the good-quality and countrywide consistent bottom-up emission information, particularly for power plants, is available. Further investigation on sources located in other regions, in particular, Europe, will be performed in the near future, with collating the corresponding bottom-up emission inventories. We have clarified this in the Sect.4 of the revised manuscript.

*More in general, could the method be applied to sources smaller than 1x10ˆ15 molec/cm$^2$ if the fit results are good? How small the source could be? Is there a minimum ratio between the source and the background, which is critical for the fitting performances? And how close the sources can be to each other to successfully perform the fit? Could you comment on these issues?*

**Response:** In general, we would agree that the method would work for smaller sources as well, if the statistics are sufficient (see e.g. Beirle et al. (2004)). But the uncertainty of the lifetime and emissions fit is much higher for smaller sources.

Thus, we dismissed the very small sources by applying a threshold of $1\times10^{15}$ molec/cm$^2$ in order to assure the reliability of the fitted results, and avoid systematic biases due to potential spatially varying artefacts in spectral analysis or the calculation of AMFs.

As for the distance between sources, we performed a sensitivity analysis, which is included as a new section (Sect. 4 of the supplement), as follows:

"As for the distance between sources, we find that it is not critical for the fit of lifetime, as the actual distribution of sources is appropriately accounted for by *C(x)*. But for the fit of the total mass, a decision of the extent of the source under investigation has to be made. Here, we define the extent of the city to be $\pm$20 km and integrate the calm VCDs in across-wind direction over this interval. Thus, any interference within 20 km will automatically be assigned to the source of interest.

We performed a sensitivity analysis to investigate the effect of the distance between sources on the estimate of emissions. We simulated the line densities of a single source with emissions of 500 molec-$NO_2$/s and with an additional source with emissions of 10%, 25% and 100% of the source of interest at 0–50 km distance, respectively, assuming an a-priori lifetime of 3 hours with a spatial smoothing following a Gaussian function with a standard deviation of 10 km. We then performed a non-linear least-squares fit of the modified Gaussian function *g(x)* (Eq.(5)) to the synthetic line densities, as illustrated in Fig. S7.

Generally, the fit cannot distinguish the source and the interference within 20 km, which tries to "explain" the interference by a larger emission. In the examples shown in Fig.S7, a 10%–100% of interference results in emission estimates which generally include the interfering source. From a distance of 30 km on, the performance of the fit gets more and more unstable, due to the interference. For distances of 40 km (and larger), the fit works properly again with a bias of less than 5% for most cases, and correctly separates the source of interest from the interfering source.

However, if the interference is comparably large as the source (500 molec-$NO_2$), uncertainties are large. Thus, we conclude that our method generally is applicable for regional dominant sources within about a radius of 100 km. Interfering sources within 20 km cannot be separated, but will be included in the emission estimate. From 40 km on, interfering sources will not be included. ”

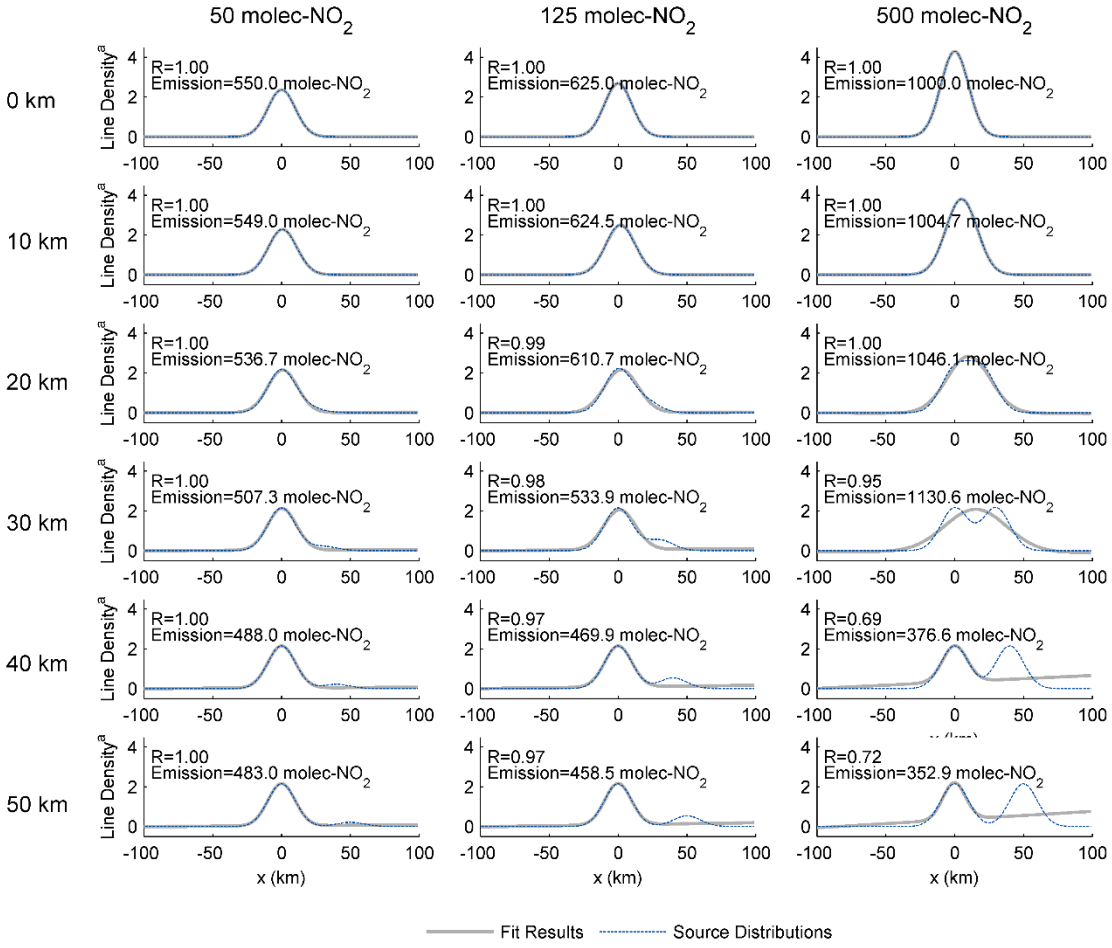


Figure S7. Sensitivity of the fitted emission to the distance between sources. Blue dot: synthetic line densities of a single source with emissions of 500 molec-$NO_2$/s under calm wind condition and with an additional source with emissions of 50, 125 and 500 molec-$NO_2$/s (from left to right) at 0–50 km (from top to bottom). Grey: emission fit based on *g(x)* (Eq. 5). The number indicates Emission resulting from the least-squares fit with 95% CI.

[a]Line Density: $NO_2$ line density ($10^{23}$ molec/cm)

*Technical corrections*

*P25197 L14 explaintion -> explanation*

**Response:** Done.

*Fig. S4 The yellow color chosen for spring and autumn are very similar, especially in a very busy figure like this is. Maybe you could replace the autumn yellow with something closer to lime or green? Or any other color you can distinguish a bit better?*

**Response:** Thanks. We have revised the figure accordingly.

*References section Several references (for example Butler et al., Gu et al., Levelt et al., Martin et al., Richter et al.) have the title not starting with a capital letter: you might want to check through. I think they should go with capital letter.*
**Response:** Thanks. We have checked through and revised the references accordingly.

## Reference

Beirle, S., Platt, U., von Glasow, R., Wenig, M., and Wagner, T.: Estimate of nitrogen oxide emissions from shipping by satellite remote sensing, Geophys. Res. Lett., 31, L18102, doi: 10.1029/2004GL020312, 2004.

Veefkind, J. P., Aben, I., McMullan, K., Förster, H., de Vries, J., Otter, G., Claas, J., Eskes, H. J., de Haan, J. F., Kleipool, Q., van Weele, M., Hasekamp, O., Hoogeveen, R., Landgraf, J., Snel, R., Tol, P., Ingmann, P., Voors, R., Kruizinga, B., Vink, R., Visser, H., and Levelt, P. F.: TROPOMI on the ESA Sentinel-5 Precursor: A GMES mission for global observations of the atmospheric composition for climate, air quality and ozone layer applications, Remote Sens. Environ., 120, 70–83, 2012.

Anonymous Referee #3

*The manuscript introduces a creative way of quantifying the $NO_x$ emissions from the satellite $NO_2$ retrievals for both power plant and urban sources located in the polluted background. It is well written and includes the detailed discussion on uncertainties in the developed method. I recommend publication of this manuscript after revisions based on the comments below. Since the manuscript can mislead the readers and future studies, careful revisions and another review of the revised manuscript may be necessary.*

**Response:** We thank Referee #3 for the comments. We addressed the comments carefully as below.

*The strength of this paper is the new method applicable to the sources in the polluted background. However, due to uncertainties in the estimated emissions from this method, the assessments of the bottom-up emission inventories with respect to the emissions in this study should be documented more carefully. For an example, the statement in the abstract, "Global inventory significantly underestimated NOx emissions in Chinese cities, most likely due to uncertainties associated with downscaling approaches" assumes that the emissions in this study are accurate. The emissions in this study from power plants are compared with the ones from CPED or eGRID, which is used as a strong support for excellent performances of the method. Looking at Figure 7, the agreement between the emissions in this study and the bottom-up inventories is not satisfactory, especially for the US, and numbers of power plants used are limited. Improved methodologies to derive the bottom-up emission inventory, MEIC are highlighted. But it does not guarantee accurate resulting emissions.*

**Response:** We recognize the general concern raised by the reviewer and fully agree that the emissions derived in this study, as well as those provided by bottom-up inventories are subject to uncertainties. In this study, we try to quantify the uncertainties of our method as best as possible, and we have extended the uncertainty discussion in the revised paper accordingly.

Bottom-up emission inventories, developed by different researchers, often differ significantly from each other, due to the application of various assumptions and extrapolations associated with the limited knowledge of activity data and emission factors. The method developed in this study provides a top-down estimate which can be used for an independent evaluation of bottom-up inventories.

Concerning the comparison of our emission estimates with eGRID for power plants in the US, we consider the agreement to be not perfect, of course, but rather good (within 50% for all power plants, which is well within the estimated uncertainties). A larger number of included power plants would of course be desirable, but we carefully defined automated selection criteria where our method yields robust emission estimates.

We agree that the accuracy of urban emissions in MEIC is probably not as good as that of emissions from power plants. However, MEIC included multiple in-house

high-resolution databases, which is expected to improve the accuracy of emission estimates. In addition, the accuracy of MEIC has been validated by extant researches, e.g., Ding et al. (2015). We thus consider it as state-of-the-art bottom-up emission inventory, and well suited for a comparison to our top-down estimates.

*In addition, errors in the ECMWF wind speed were not discussed in the manuscript. Table S3 in the supplementary material shows overestimated wind speed in ECMWF, which could underestimate $NO_x$ lifetime and increase the estimated emission rate.*

**Response:** Thanks. We have emphasized the discussion on effect of uncertainties of wind speeds on fitted results in Sect.3 of the supplement, as follows:

"We carried out a comparison of wind information between ECMWF and sounding measurements (Table S3). Here we focus on the comparison of the quantity used for the lifetime estimate, i.e. the projected wind components for each wind direction sector. We firstly sorted ECMWF wind fields for the years 2005–2013 into 8 wind direction sectors and classified the simultaneous sonde data into the same wind direction sector, and then calculate the mean of the projected wind speeds from both datasets to compare. While *total* wind speeds from ECMWF and sonde measurements agree quite well (~5% on average for wind speeds>2 m/s), the *projected* wind components are systematically higher for ECMWF. This can be expected, as ECMWF wind fields are the basis for the wind direction classification. If, for instance, the true wind would be 5 m $s^{-1}$ from north, but the model wind is 5 m $s^{-1}$ from east, the case is classified as easterly, while the actual easterly wind component is 0. That is, deviations of the wind direction (even if 0 on average) cause a systematic bias due to this projection procedure. Thus, the deviation of the projected wind speeds covers uncertainties of the sorting procedure caused by deviations of the wind direction, and allow for an estimate of the overall uncertainty due to wind fields. The deviations for non-mountainous sites are, on average, acceptable (26%). Note also that de Foy et al. (2015) report on ERA-Interim winds yielding a better lifetime estimate compared to the North American Regional Reanalysis project (NARR). For mountainous sites, however, significantly higher deviations are found (37% on average) due to insufficient spatial resolution of ECMWF (see also Sect. 2.6 of the manuscript). **"**

*To evaluate the method thoroughly, extensive validations of the developed emission estimations (and bottom-up emission inventories) utilizing independent data set and/or regional chemical transport models will be required.*

**Response:** We consider our manuscript as proposal of a new method for top-down emission estimates of $NO_x$ in polluted background, which was not possible with previous methods. We carefully discussed and quantified the uncertainties of our method, and extended the revised manuscript in this respect. Of course, further evaluation of the performance of our method with independent data sets and regional CTMs would be desirable, but is beyond of this conceptual study. We feel that using CTMs is a good plus, but not necessary for this work. In fact, in many previous published studies which used Gaussian fitting models to derive emissions, CTMs are not involved (e.g., Beirle et al., 2011; Fioletov et al., 2011; Lu et al., 2015).

We would like to point out, however, that our method provides an independent emissions quantification approach for the comparison to, and validation of, bottom-up inventories without involvement of CTMs.

*Regarding the method developed in this study, the background level of $NO_2$ ($\varepsilon_i+\beta_i x$) can have information on the emissions from the source of interest since the lifetime of $NO_2$ is much shorter than relatively passive scalars such as CO and $CH_4$.*

**Response:** Our method aims for emission estimates of local sources in generally polluted regions. Thus, we cannot estimate the emissions directly from the absolute measured tropospheric column, but have to account for the "background". In a first approach, we have just fitted Gaussian functions plus a constant offset to *C(x)*, which, however, often is not sufficiently reflecting the observed spatial patterns for calm winds. We thus added one further parameter, i.e. a spatially variable (linear) background, as the simplest possible expansion of the model function, which improved the performance of the fit significantly in many cases.

The reason for the need of a spatial variation of the background is related to the spatial distribution of sources, which is often not symmetric, and a possible gradient in the upper tropospheric $NO_2$.

*In addition, the chemical lifetime defined in this study is an e-folding time. Whether the lifetime can be directly used for derivation of emission rate without application of an empirical coefficient or a weighting factor is a question.*

**Response:** In this study, we assumed that the removal of $NO_2$ can be simply described by a first order loss, and thus the chemical decay of $NO_2$ follows an exponential decay function *e(x)* (Eq. 2) with an e-folding distance $x_0$, which yields an overall, effective lifetime $\tau$. From the good lifetime fit performance, we see no indications that this assumption is insufficient.

In Beirle et al. (2014), it was investigated how far the estimated lifetime by this approach might be biased in case of temporal fluctuations of both emissions and instantaneous lifetimes. The impact of such fluctuations was found to be rather small. In the revised paper, we briefly discussed this effect in section 2.2.2.

## Reference


Beirle, S., Boersma, K. F., Platt, U., Lawrence, M. G., and Wagner, T.: Megacity emissions and lifetimes of nitrogen oxides probed from space, Science, 333, 1737–1739, 2011.

Beirle, S., Hörmann, C., Penning de Vries, M., Dörner, S., Kern, C., and Wagner, T.: Estimating the volcanic emission rate and atmospheric lifetime of SO2 from space: a case study for Kīlauea volcano, Hawai'i, Atmos. Chem. Phys., 14, 8309–8322, doi:10.5194/acp-14-8309-2014, 2014.

Ding, J., van der A, R. J., Mijling, B., Levelt, P. F., and Hao, N.: $NO_x$ emission estimates during the 2014 Youth Olympic Games in Nanjing, Atmos. Chem. Phys., 15, 9399–9412, 10.5194/acp-15-9399-2015, 2015.

Fioletov, V. E., McLinden, C. A., Krotkov, N., Moran, M. D., and Yang, K.: Estimation of SO2 emissions using OMI retrievals, Geophys. Res. Lett., 38, L21811, doi:10.1029/2011gl049402, 2011.

Lu, Z., Streets, D. G., de Foy, B., Lamsal, L. N., Duncan, B. N., and Xing, J.: Emissions of nitrogen oxides from US urban areas: estimation from Ozone Monitoring Instrument retrievals for 2005–2014, Atmos. Chem. Phys., 15, 10367-10383, doi:10.5194/acp-15-10367-2015, 2015.

Anonymous Referee #4

*Overall an interesting and relevant paper. The data are well presented, the measuring and analysis methods seems to me sound although the many fitting, scaling and filtering functions used under different situations with different areal extend makes me confused from time to time.*

**Response:** We thank Referee #4 for the comments. In order to avoid confusion, we tabulated the fit intervals for lifetime and emission fits in a new Table 1 of the revised manuscript.

*The authors state that the mean lifetime is derived from the change of the observed $NO_2$ patterns under windy vs. calm conditions. But if I understand the text well enough, N is derived from C and C is the line density under calm wind only as states into the text (near Eq 4). So this would be the blue lines in Figure 2 since these are the line densities for calm winds? In the figure caption on the contrary, N is fitted to the windy conditions for the different wind sectors (grey line on red crosses). Please clarify, since I am confused.*

**Response:** The basic idea of the method is that patterns of line densities under windy conditions result from the transport, chemical decay and spatial smoothing of emission patterns. We used the line density under calm conditions, *C(x)*, as the proxy of emission patterns and performed a non-linear least-squares fit of *N(x)* (Eq. 4) to the observed $NO_2$ patterns under windy conditions, with the observed *C(x)* as fixed input and $x_0$, $a$ and $b$ as fit parameters. Thus, we state that results are derived from the change of the observed $NO_2$ patterns under windy versus calm conditions. We have clarified this in Sect.2.2.2 of the revised manuscript, as follows:

"The patterns of line densities under windy conditions result from the transport, chemical decay and spatial smoothing of emission patterns. The basic idea is to use the $NO_2$ patterns observed under calm conditions, *C(x)*, as proxy of emission patterns instead of assuming a single point source as in previous studies. Lifetime information is then gained based on the observed change of the $NO_2$ patterns under windy versus calm conditions."

*It is also not clear to me why you subtract wind speeds between windy and calm conditions for use in deriving the life time. If it is not of a big effect as stated in the footnote 1 why bother?*

**Response:** As the mean wind speed for the selection of days classified as calm is low, but not zero, line density under calm wind conditions *C(x)* is already shifted with respect to the emission pattern. In our study, the correction of this effect (i.e. taking the wind speed offset to calm conditions) is only marginal (so we put it in a footnote). However, we still would like to discuss this systematic effect in the manuscript as a general characteristic of our method; for different conditions (e.g. if a higher threshold for calm is chosen and wind directions are persistent), this effect might actually become significant.

*The $NO_2$ amount A on top of the background is determined by fitting the functions $g_i(x)$ simultaneously for all available wind directions. What do the authors mean with" simultaneously"? Do they mean that they fit it for the 8 different wind sectors at the same time and still only retrieve one A? Please rephrase and clarify.*

**Response:** We have rephrased this in Sect.2.2.3 of the revised manuscript, as follows:
"While the e-folding distance is fitted for each wind direction separately (and mean lifetimes might actually be different for each wind direction), the emissions are not expected to depend on wind direction. We thus use all available wind directions to perform one fit of all functions $g_i(x)$ simultaneously with wind sector dependent backgrounds, but one overall parameter *A*."

*The possible linear gradient in the back ground of Equation 5: how can this be explained? Is it also possible that it results from interannual trends in the emissions over the area for the $NO_2$ period under investigation?*

**Response:** Our method aims for emission estimates of local sources in generally polluted regions. Thus, we cannot estimate the emissions directly from the absolute measured tropospheric column, but have to account for the "background". In a first approach, we have just fitted Gaussian functions plus a constant offset to $C(x)$, which, however, often is not sufficiently reflecting the observed spatial patterns for calm winds. We thus added one further parameter, i.e. a spatially variable (linear) background, as the simplest possible expansion of the model function, which improved the performance of the fit significantly in many cases.
The reason for the need of a spatial variation of the background is related to the spatial distribution of sources, which is often not symmetric, and a possible gradient in the upper tropospheric $NO_2$.

*The fit interval h is not well introduced in the main text. Suddenly it pops up. Please clarify.*

**Response:** We have clarified this in Sect.2.2.3 of the revised manuscript, as follows:
"The fit of total $NO_2$ mass is performed over the interval *h* in wind direction (see Fig. S2)."

*L26, P24189: replace "division" by "dividing". L9, P24192: should be "visually inspection".*

**Response:** Thanks. We have revised the manuscript accordingly.

*Figure 5: Why not using the same color bar range for both panels to stress the difference in total $NO_2$ columns between China and US?*

**Response:** Thanks. We have chosen the same color bar for $NO_2$ TVCDs for both China and the US in the revised manuscript.

# $NO_x$ lifetimes and emissions of cities and power plants in polluted background estimated by satellite observations

**F. Liu[1,2,3], S. Beirle[3], Q. Zhang[2], S. Dörner[3], K. B. He[1,2], and T. Wagner[3]**

[1]{State Key Joint Laboratory of Environment Simulation and Pollution Control, School of Environment, Tsinghua University, Beijing 100084, China}

[2]{Ministry of Education Key Laboratory for Earth System Modeling, Center for Earth System Science, Tsinghua University, Beijing 100084, China}

[3]{Max-Planck-Institut für Chemie, Mainz 55128, Germany}

Correspondence to: S. Beirle (steffen.beirle@mpic.de)

Q. Zhang (qiangzhang@tsinghua.edu.cn)

## Abstract

We present a new method to quantify $NO_x$ emissions and corresponding atmospheric lifetimes from OMI $NO_2$ observations together with ECMWF wind fields without further model input for sources located in polluted background. $NO_2$ patterns under calm wind conditions are used as proxy for the spatial patterns of $NO_x$ emissions, and the effective atmospheric $NO_x$ lifetime is determined from the change of spatial patterns measured at larger wind speeds. Emissions are subsequently derived from the $NO_2$ mass above background integrated around the source of interest.

Lifetimes and emissions are estimated for 17 power plants and 53 cities located in non-mountainous regions across China and the US. The derived lifetimes are 3.8 ± 1.0 hours (mean ± standard deviation) on average with ranges of 1.8 to 7.5 hours. The derived $NO_x$ emissions show generally good agreement with bottom-up inventories for power plants and cities. Regional inventory shows better agreement with top-down estimates for Chinese cities compared to global inventory, most likely due to different downscaling approaches adopted in the two inventories.

# 1 Introduction

Nitrogen oxides ($NO_x$) are toxic air pollutants and play an important role in tropospheric chemistry as precursors of tropospheric ozone and secondary aerosols (Jacob et al., 1996; Seinfeld and Pandis, 2006). Power plants and cities with large vehicle populations and intense industrial activities are significant anthropogenic emitting sources of $NO_x$. Accurate knowledge of $NO_x$ emissions on urban scales is thus a critical factor for accurate bottom-up emission inventories, which are important inputs for chemical transport models (CTMs) and for the development of mitigation strategies.

Bottom-up emission inventories depend on information of fuel consumptions and emission factors, which are subject to substantial uncertainties (Butler et al., 2008; Zhao et al., 2011). A significant improvement in accuracy of emission inventories for power plants has been achieved by the installation of continuous emissions monitoring systems (CEMS). For example, in the US, under the 1990 Clean Air Act, power plant operators are required to install an automated data acquisition and handling system for measuring and recording pollutant concentrations from plant exhaust stacks and follow the monitoring regulations to ensure that the reported emission data is consistent and of high quality (Kim et al., 2009). For countries where reliable CEMS data is not available (like China), activity rates and emission factors can be adopted at plant-level to improve the accuracy of power plant emissions (e.g. Zhao et al., 2008; Liu et al., 2015). But developing emission inventories for individual cities with high accuracy faces enormous challenges, considering the lack of a complete and reliable database including fuel consumptions and emission factors at city level. Emissions at city level are often downscaled from regional emission estimates, based on surrogates (e.g. population density, industrial productivity, and etc.), which however often just roughly reflect the magnitude and spatial distribution of urban emissions. Thus, independent emission estimates would be a desirable complement to validate and improve existing emission inventories.

The $NO_2$ tropospheric vertical column densities (TVCD, the vertically integrated concentration in the troposphere) retrieved from satellite measurements provide valuable global information on the spatio-temporal patterns of $NO_x$, including trends (e.g., Richter et al., 2005; Schneider and van der A, 2012; Hilboll et al., 2013), responses of $NO_2$ level changes to air quality control as well as economic and political factors (e.g., Duncan et al., 2013; Lelieveld et al., 2015), and temporal variations like weekly cycles in $NO_2$ TVCDs (Beirle et al, 2003; Russell et al., 2010; Valin et al., 2014). In addition, the satellite $NO_2$ measurements have been applied to quantify $NO_x$ emissions. In a pioneering study (Leue et al., 2001), the downwind decay of $NO_2$ TVCDs in continental outflow regions was used to estimate a (constant) $NO_x$ lifetime, which was then applied to project global $NO_x$ emissions from the measured mean $NO_2$ TVCDs. Later on, CTMs were employed to exploit satellite observations as a constraint towards improving $NO_x$ emission inventories (e.g., Martin et al., 2003; Konovalov et al., 2006; Kim et al., 2009; Lamsal et al., 2011). The derived top-down inventories show pronounced differences relative to bottom-up estimates and their accuracy has been validated by the improved performance of model simulations with respect to in-situ measurements (e.g., Martin et al., 2006). However, the top-down inventories are usually determined at regional/global scale related to the spatial resolution of CTMs, while the spatial scales relevant for individual emission hotspots (power plants or cities) are not resolved. In addition, modelled lifetimes have large uncertainties (Lin et al., 2012) due to the highly non-linear small-scale chemistry in urban areas, and are thus probably not appropriate for relating $NO_2$ TVCDs to $NO_x$ emission rates at city level.

With the launch of the Ozone Monitoring Instrument (OMI) (Levelt et al., 2006) with high spatial resolution (13×24 $km^2$ at nadir), individual large sources like Megacities and power plants can be resolved. In a recent study, Beirle et al. (2011) averaged OMI $NO_2$ measurements separately for different wind directions, thereby constructing clear downwind plumes which allow a simultaneous fit of the effective $NO_x$ lifetimes and emissions, without the need of a chemical model. Valin et al. (2013) adopted this

approach, but rotated satellite $NO_2$ observations according to wind directions such that all the $NO_2$ columns are aligned in one direction (from upwind to downwind). The rotation procedure accumulated a statistically significant data set to examine the dependence of $NO_x$ lifetime on the wind speed. Following studies e.g. de Foy et al. (2015) and Lu et al. (2015) adopted this plume rotation technique and quantified $NO_x$ emissions from isolated power plants and cities over the US respectively, which showed that the method can give reliable estimates over multi-annual averages and even provide estimates of emission trends with reasonable accuracy. de Foy et al. (2014) also analyzed the performance of the method using model simulations with fixed *a priori* lifetimes and realistic wind data, which proved that the fitted results were accurate in general and showed best performance for strong wind cases. Alternative approaches based on model functions with multiple dimensions, e.g. a two dimensional Gaussian functions (Fioletov et al., 2011) and a three dimensional function (Fioletov et al., 2015), were also proposed to estimate lifetimes and emissions.

However, so far all studies assume that the source of interest can be considered as a "point source", which works well for isolated sources like e.g. the city of Riyadh, showing a high contrast against clean background with small and smooth TVCDs. However, for sources located in a heterogeneously polluted background, a modification of these methods is needed in order to account for the effect of interfering sources within small distances.

In this work, we present a new method for the quantification of $NO_x$ lifetimes and emissions for power plants and cities located in polluted background. The mean OMI $NO_2$ distribution for 2005−2013 is calculated separately for calm conditions as well as for different wind direction sectors according to ECMWF (European Center for Medium-range Weather Forecast) wind fields. The mean lifetime is derived from the change of the observed $NO_2$ patterns under windy versus calm conditions. $NO_x$ emissions of power plants and cities over China and the US are subsequently

quantified from the integrated TVCDs and the derived lifetimes, and compared to bottom-up emission inventories.

# 2 Methodology

## 2.1 Satellite $NO_2$ data

We base this study on $NO_2$ TVCDs from the OMI tropospheric $NO_2$ (DOMINO) v2.0 product (Boersma et al., 2011), which is provided by the Tropospheric Emissions Monitoring Internet Service (TEMIS, http://www.temis.nl). OMI is a UV-VIS nadir-viewing satellite spectrometer (Levelt et al., 2006) on board the Aura satellite (Celarier et al., 2008), launched in 2004. $NO_2$ columns are derived from radiance measurements, using the Differential Optical Absorption Spectroscopy (DOAS) algorithm (Platt, 1994). OMI provides daily global coverage with a local equator crossing time of approximately 13:45 pm. It detects radiance spectra from 60 across-track pixels with ground pixel sizes ranging from 13×24 $km^2$ at nadir to about 13×150 $km^2$ at the outermost swath angle (57°).

The 10 outermost pixels on both sides of the swath are excluded in this study to limit the across-track pixel width <40 km. From June 2007, OMI has shown severe spurious stripes, known as row anomalies that are likely caused by an obstruction in part of OMI's aperture (http://www.knmi.nl/omi/research/product/rowanomaly-background.php). The affected pixels are also excluded from the analysis. Only mostly cloud free observations (effective cloud fraction <30%) are considered in this study.

Mean $NO_2$ TVCDs over the US and China during "ozone season" (May-September) for 2005 to 2013 are calculated separately for calm (wind speed below 2 m/s) and 8 different wind direction sectors following the approach in Beirle et al. (2011). We focus on the ozone season to include the photochemically relevant months for ozone production (USEPA, 2014) and to exclude the winter data with larger uncertainties due to larger solar zenith angles, variable surface albedo (snow), and longer $NO_x$ lifetime. Wind fields at a lat/long grid of 0.36° width are taken from the ECMWF

ERA interim reanalysis (Dee et al., 2011), and the horizontal wind components of the lowermost 500 m are averaged. Individual clear-sky observations of $NO_2$ TVCDs are assigned to a 2×finer grid (0.18°, comparable to the extent of OMI ground pixels) according to the pixel center coordinates, and associated with the corresponding ECMWF wind fields interpolated in time.

## 2.2 $NO_2$ outflow models and lifetime/emission fits

In this section, we present a modified method compared to Beirle et al. (2011) for the determination of lifetimes and emissions for complex source distributions. The basic idea is to use the measured $NO_2$ spatial pattern under calm wind conditions as proxy for the distribution of $NO_x$ sources, instead of assuming a single point source.

Below, we (a) summarize the fitting procedure of Beirle et al. (2011) and demonstrate that this method cannot be applied for multiple sources (Sect. 2.2.1), (b) describe the model function for the modified lifetime fit (Sect. 2.2.2), and (c) eventually explain how emission rates are determined (Sect. 2.2.3).

We select Harbin (45.8°N, 126.7°E), the capital of Heilongjiang province in China, with a population of about 6 million (city) to 10 million (greater area) inhabitants, to demonstrate our approach. Harbin is a typical city located in polluted background, surrounded by three other large $NO_x$ sources (i.e. the cities of Daqing, Jilin and Changchun) within ~200 km radius. Figure 1 displays mean $NO_2$ TVCDs around Harbin for calm conditions (a), southerly wind (b) and their difference (c). The outflow plume of $NO_2$ from Harbin is not as clear as that from isolated sources (e.g. Riyadh in Beirle et al. (2011)), due to the interferences from surrounding sources. But the spatial pattern of their difference (Fig. 1c) still clearly reveals outflow patterns, consistent with ECMWF wind fields.

In order to investigate the downwind plume evolution, 1-dimensional $NO_2$ "line densities", i.e. $NO_2$ per cm, are calculated as function of distance for each wind direction sector separately by integration of the mean $NO_2$ TVCDs (i.e. $NO_2$ per $cm^2$) perpendicular to the wind direction, as in Beirle et al. (2011).

### 2.2.1 Isolated point source outflow model: Lifetime and Emissions

In Beirle et al. (2011), a simple model function *M(x)* (Eq. (1)) was used to fit the observed line densities, which is composed of an exponential function *e(x)* (Eq. (2)) describing the transport pattern and chemical decay, and a Gaussian function *G(x)* (Eq. (3)) accounting for different effects causing spatial smoothing (e.g., the spatial extent of the source, the OMI ground pixel size, or wind fluctuations).

$$M(x) = E \times (e \otimes G)(x) + B \quad (1)$$

$$e(x) = \exp\left(-\frac{x - X}{x_0}\right) \quad \text{for } x \geq X, \text{ 0 otherwise} \quad (2)$$

$$G(x) = \frac{1}{\sqrt{2\pi}\sigma}\exp\left(-\frac{x^2}{2\sigma^2}\right) \quad (3)$$

*E* represents total emissions, *B* represents a constant background; *X* is the location of the source (relative to the a priori co-ordinates of the site under investigation), $x_0$ is the e-folding distance downwind; and $\sigma$ is the standard deviation of *G(x)*. The mean lifetime $\tau$ is derived from the e-folding distance $x_0$ by division by *w*, the mean projected wind speed. By this approach, emissions and lifetimes of $NO_2$ are fitted simultaneously.

Uncertainties are estimated from the confidence intervals of individual fits, the variability of fit results of the same location for different wind directions, and the dependency of *a priori* assumptions like fit intervals and the detailed choice for the applied wind data, as inferred from sensitivity studies (see the supplementary online material of Beirle et al., 2011, for details). In addition, the uncertainty of $NO_2$ VCDs of about 30% is transmitted to the final emission estimate. Final errors are of the order of 50% for lifetimes, and 60% for emissions, with (i) the fit uncertainty, (ii) the uncertainties introduced by the applied wind data, and (iii) uncertainties for VCDs (affecting only the emission estimate) being the most important contributions.

In Beirle et al. (2011) lifetime and emissions are derived for nine isolated hot spots exhibiting high $NO_2$ TVCDs over a clean background within about 200 kilometers.

But this method cannot be applied to hot spots surrounded by additional significant sources, like Harbin (Fig. 1), as by definition, the method can only represent a single "point source" convolved with a Gaussian function. For instance, an additional source at 100 km with only 10% of the emissions of the source under investigation causes a lifetime bias of ~20 %, as the fit tries to "explain" increased downwind values by a longer lifetime (see Fig. S1 and explanations in the supplement). For an interfering source of the same order as the source of interest, the method fails completely.

### 2.2.2 Mixed source outflow model: Lifetime

We develop an alternative method accounting for emissions from multiple sources. The patterns of line densities under windy conditions result from the transport, chemical decay and spatial smoothing of emission patterns. The basic idea is to use the $NO_2$ patterns observed under calm conditions, $C(x)$, as proxy of emission patterns instead of assuming a single point source as in previous studies. Lifetime information is then obtained based on the observed change of the $NO_2$ patterns under windy versus calm conditions. Note that the 1-D pattern of line densities under calm conditions has to be determined along the same (wind) direction, for which the line densities under windy conditions are determined. That means that in total eight 1-D line densities under calm conditions are determined for the eight wind directions. However, only directions with reasonable reliability are considered where mean $NO_2$ line densities for both calm and windy conditions are well defined (i.e., gaps due to missing data are less than 10% in the across-wind integration interval $i$ and less than 20% in the fit interval in wind direction $f$). We define the new model function $N(x)$ as:

$$N(x) = a \times [e \otimes C](x) + b \quad (4)$$

where $e(x)$ is again a truncated exponential function (Eq. (2) with $X = 0$). The scaling factor $a$ and offset $b$ are included to account for possible systemic differences between windy and calm wind conditions (e.g. cloud conditions, vertical profiles, or lifetimes), which will be discussed in Sect. 3.1 in detail.

We perform a non-linear least-squares fit of $N(x)$ to the observed line densities with $a$, $b$, and $x_0$ as fitting parameters. We set the fit interval in wind direction $f$ to 600 km (300 km in downwind direction, which corresponds to 3 times of the e-folding distance for a lifetime of 5 hours and a mean wind speed of 6 m/s). The across-wind integration interval $i$ is set to be half (300 km). $f$ and $i$ are indicated in Fig. 1a and Fig. 1b. The intervals are larger than those in Beirle et al. (2011), since not only the source under investigation, but also interfering sources have to be appropriately accounted for when comparing line densities of calm and windy conditions. We also perform fits with different intervals (±100 km, see Table S1) and find only small changes (~10%) for the resulting lifetimes.

Figure 2a displays the observed line densities for calm (blue) and southerly winds (red) around Harbin, and the fitted model function $N(x)$ (grey). Generally, $N(x)$ describes the observed downwind patterns well: the coefficients of determination ($R^2$) between observation and fit are 0.96–0.99 with the range of 3.0–4.4 hours for different wind directions, as shown in Fig. 2a-e.

Like in Beirle et al. (2011), the lifetime $\tau$ is derived by the ratio of the fitted e-folding distance and the mean wind speed[1]: $\tau = x_0/w$. For Harbin, $\tau$ is computed to be 3.9 hours with a typical 95% confidence interval (CI) of ±0.6 hours for southerly winds. Averaging the fit results for all wind direction sectors with a good fit performance (i.e. R >0.9, lower bound of CI >0, and CI width <10 h,) yields $\tau$ = 3.5 hours with a standard deviation of 0.6 hours (Fig. 2), using the fit residues as well as the CI of $\tau$ as inverse weights, as in Beirle et al. (2011).

---

[1]Note that we subtracted the residual mean wind speed under calm wind conditions from $w$ in order to account for the subtle movement of $C(x)$ compared to the emission pattern; this is, however, a small effect (the relative change between $\tau$ determined by wind speeds with and without subtracting calm wind speeds is within -2%~3%). But the effect could be larger for persistent winds and for larger thresholds for calm.

Here we assumed that the removal of $NO_2$ can be simply described by a first order loss, and thus the chemical decay of $NO_2$ follows an exponential decay function *e(x)* (Eq. (2)) with an e-folding distance $x_0$, which yields an overall, effective lifetime $\tau$. In Beirle et al. (2014), it was investigated how far the estimated lifetime by this approach might be biased in case of temporal fluctuations of both emissions and instantaneous lifetimes. The impact of such fluctuations was found to be rather small.

### 2.2.3 Mixed source outflow model: Emissions

The modified fitting function *N(x)* proved to be capable of gaining lifetime information even for complex source distributions. The interferences from multiple neighboring sources, which cannot be represented by a single-source Gaussian distribution, are successfully described by the new model function using *C(x)* as proxy for the spatial distribution of $NO_x$ sources. However, in contrast to the previous fitting function *M(x)* in Beirle et al. (2011), *N(x)* does not contain the magnitude of $NO_x$ emissions directly, but only the emission pattern represented by $NO_2$ under calm conditions. Thus, total $NO_x$ emissions have to be estimated separately.

According to mass balance, the total mass of $NO_x$ equals the emission rate times lifetime. Emissions can thus be derived in a three-step approach by (a) integrating observed TVCDs originating from the source of interest to calculate the total mass of $NO_2$, (b) scaling $NO_2$ to $NO_x$, and (c) division by the lifetime $\tau$, which was derived as described in the previous section.

(a) Total $NO_2$ mass

In order to quantify the total $NO_2$ mass of the target source, the observed TVCDs have to be integrated around the source, in which (1) interferences with neighboring sources have to be avoided and (2) a polluted background has to be appropriately accounted for. Thus, we base the estimation of the total $NO_2$ mass on the mean TVCDs under calm conditions, to minimize interferences by advection. Again, we

calculate line densities by integrating the $NO_2$ TVCDs in "across-wind" direction[2], but for a smaller interval *v* representing the spatial extent of megacities or urban centers, but exclude neighboring sources. Here we define *v*=40 km.

We then perform a non-linear least-squares fit of a modified Gaussian function *g(x)* to these line densities under calm wind condition, as illustrated in Fig. 3. The line densities integrated perpendicular to the different wind direction sectors are used to constrain the fitted *A* in *g(x):*

$$g_i(x) = A \times \frac{1}{\sqrt{2\pi}\sigma_i} \exp\left(-\frac{(x-X)^2}{2\sigma_i^2}\right) + \varepsilon_i + \beta_i x \qquad (5)$$

*i* represents the wind direction sector. Note that the projections of line densities under calm wind conditions for opposite wind direction sectors, e.g., north and south, are just mirrored. Thus, we combined the projections for opposite wind direction sectors. That is, *i* represents Southeast-Northwest, South-North, Southwest-Northeast and East-West respectively. *X* is the location of the source (relative to the a priori co-ordinates of the site under investigation). $\sigma_i$ is the standard deviation of the Gaussian $g_i(x)$, and $\varepsilon_i$ and $\beta_i$ represent an offset and a possible linear gradient in the background field respectively. While the e-folding distance is fitted for each wind direction separately (and mean lifetimes might actually be different for each wind direction), the emissions are not expected to depend on wind direction. We thus use all available wind directions to perform one fit of all functions $g_i(x)$ simultaneously with wind sector dependent backgrounds, but one overall parameter *A*.

The $NO_2$ amount *A* (in molecules) around the source on top of the (wind sector dependent) background is determined by fitting the functions $g_i(x)$ simultaneously for all available wind directions.

The fit of total $NO_2$ mass is performed over the interval *h* in wind direction (see Fig. S2). The fit interval *h* has to be chosen to be larger than *v* in order to allow for a meaningful fit of *g(x)*. We set *h* to 200 km for cities (see Fig. S2) and 100 km for

[2]Though focussing on calm conditions, we calculate the projections for different wind direction sectors analogue to the lifetime fit procedure.

power plants respectively. The fit interval thus potentially includes interfering sources. However, these interferences are in first order accounted for by the linear variation of the background fitted in function $g_i(x)$. Note that the fit $g(x)$ is less sensitive to interfering sources compared to the original fit of $M(x)$ in Beirle et al. (2011), as lifetime is not involved here.

The small interval $v$ (40 km) excludes neighboring sources, but does not capture the full plume in across wind direction due to dilution. This effect is corrected for by scaling $A$ afterwards by a factor $f(\sigma_i)$ based on the fitted plume width $\sigma_i$:

$$f(\sigma_i) = \int_{-20km}^{20km} \frac{1}{\sqrt{2\pi}\sigma_i} \exp\left(-\frac{(x-X)^2}{2\sigma_i^2}\right) \Big/ \int_{-\infty}^{\infty} \frac{1}{\sqrt{2\pi}\sigma_i} \exp\left(-\frac{(x-X)^2}{2\sigma_i^2}\right) \quad (6)$$

Note that we consider a larger interval (60 km for $v$ and 300 km for $h$) for Pearl River Delta, which is a megalopolis covering nine prefectures over an area of about 56,000 km$^2$. We tabulated the intervals chosen for fits for different cases in Table 1.

The resulting emissions are rather insensitive with respect to modified settings for $v$ and $h$ (see supplement, Sect. 3). Again, fit results with poor performance (R <0.9, lower bound of CI <0, CI width >0.8$\times A$) are discarded.

(b) Scaling $NO_2$ to $NO_x$

According to the typical [NO]/[$NO_2$] ratio of 0.32 under urban conditions at noon (Seinfeld and Pandis, 2006), the total $NO_2$ mass is scaled by a factor of 1.32 in order to derive total $NO_x$ mass following Beirle et al. ( 2011).

(c) Emission rates ($NO_x$ amount per time unit) are derived by dividing of the total $NO_x$ mass by the lifetime derived for the respective location as described in Sect.2.2.2.

For Harbin, the total mass (in terms of $NO_2$) is computed to be $33.2\times10^{28}$ molec with a CI of $2.4\times10^{28}$ molec. The total $NO_x$ emissions derived for Harbin are 58.1 mol/s.

## 2.3 Uncertainties

We define total uncertainties of the fitted lifetimes and emissions analogue to the procedure described in Beirle et al. (2011), basically based on the fit performance and the dependencies on the a priori settings as investigated in sensitivity studies. Here we shortly list the main sources of uncertainties and how they are quantified. Further details are provided in Sect.3 of the Supplement. The resulting quantitative error estimates are given and discussed below along with the derived lifetime and emission estimates.

The confidence intervals (CIs) resulting from the least-squares fits of Eq. (4) and Eq. (5) directly reflect the uncertainties of the derived lifetimes and emissions. In addition, the standard deviations of the fitted lifetimes for different wind direction sectors provide information on the consistency of the method. Both effects can be quantified straightforward and are included in the total uncertainty, contributing about 30% for lifetimes and 20% for emissions arising from CI and less than 40% for both arising from standard mean error (see Sect.3 of supplement), respectively. The dependency on the a priori choices of integration and fit intervals are quantified based on sensitivity studies and found to be of the order of 10%.

Accurate wind fields are required for the sorting procedure as well as for the conversion of the downwind decay from a function of distance into a function of time. Again, the impact of the *a priori* settings (horizontal ECMWF wind fields vertically integrated over the lowest 500m) are estimated based on sensitivity studies. In addition, ECMWF wind fields have been checked by comparison to in-situ sonde measurements, which generally agree well, except over complex terrain (see Sect. 2.6). The comparison of projected wind speeds of from ECMWF and sonde measurements allows to estimate the uncertainty of the lifetime fit caused by uncertainties of both ECMWF wind speeds and direction. Overall, the uncertainty related to wind fields is about 30%.

In addition, the derived emissions (but not the lifetime) are affected by the uncertainty of tropospheric $NO_2$ TVCDs (30%) and the $NO_2/NO_x$ ratio (10%).

In the supplement, we also discuss sophisticated effects such as the potential dependence of lifetimes on wind conditions, the assumption of a constant $NO_2/NO_x$ ratio, and the concept of a single lifetime describing the downwind evolution of $NO_2$ over several hours. These effects have been found to be rather small.

We define total uncertainties of the resulting lifetimes and emissions as the root of the quadratic sum of the above mentioned contributions, which are assumed to be independent.

### 2.4 Bottom-up emission inventories

We use bottom-up emission inventories to pre-select promising sites and for a comparison to the derived top-down estimates. We select inventories that provide up-to date, multi-year $NO_x$ emissions at high spatial resolution and are widely used in the community. The following inventories are considered:

For power plants, we use the China coal-fired Power plant Emissions Database (CPED) developed by Liu et al. (2015) based on unit-level fuel consumptions and emission factors derived from various sources, and the US Emissions & Generation Resource Integrated Database (eGRID) using emissions derived from continuous emissions monitoring systems (available at http://www.epa.gov/cleanenergy/energy-resources/egrid/) (USEPA, 2014). For cities, we use the Multi-resolution Emission Inventory for China (MEIC: http://www.meicmodel.org) compiled by Tsinghua University, the accuracy of which has been validated by extant researches (e.g., Ding et al., 2015), and the global inventory of the Emissions Database for Global Atmospheric Research (EDGAR) v4.2 (EC-JRC/PBL, 2011) for the US.

For the comparison to the derived top-down estimates, a 8-year (2005−2012) average from CPED and a 4-year (2005, 2007, 2009 and 2010) average from eGRID for the ozone season are used for power plants, of which the uncertainties are about 30% (Liu et al., 2015) for CPED and 10% for eGRID (5% arise from continuous emissions monitoring systems (Gluck et al., 2003) and another 5% arise from yearly variations

in emissions after 2010), respectively. In addition, the mean emissions for the ozone season of the years 2005−2012 in MEIC and the mean annual emissions for the years 2005−2008 in EDGAR are used for cities, of which the uncertainty is estimated to be within a factor of 1/2 and 2 according to the MEIC and EDGAR expert judgment of "medium magnitude of uncertainty" (Olivier et al., 2002). The bottom-up urban emissions derived from regional/global inventories have larger uncertainties compared to power plant emissions, primarily arising from the low-resolution activity rates/emission factors at regional level, and the spatial allocation technique using surrogates to break regional-based emission data down to cities. Furthermore, temporal coverage of bottom-up emissions is limited, inducing additional uncertainties. For instance, a decline in $NO_2$ TVCDs from the years 2005−2008 to 2009−2013 with an average total reduction of 14 ± 9% (mean ± standard variation) is detected for investigated US cities (Fig. S3). However, the most recent year available in EDGAR v4.2 is 2008, which cannot reflect the recent decline in $NO_x$ emissions, thus overestimate the average emissions.

For the comparison of bottom-up and top-down emissions for individual sites, the power plant inventories directly represent the stack emissions of individual facilities. For total city emissions, the gridded emission inventories have to be integrated over the metropolitan area for which the proposed top-down method is sensitive. Here, we define this area as 40×40 $km^2$, consistent with the considered interval $v$ in Sect. 2.2.3. For PRD, we consider a larger interval of 120×120 $km^2$.

## 2.5 Selection of investigated sources

For this study, we choose large power plants and cities across China and the US as the pre-selected candidates, of which bottom-up emission information is available from inventories described above. Power plants with $NO_x$ emission rates greater than 10 Gg/yr (CPED/eGRID) are investigated. Power plants located in urban areas (100 km around city centers) are excluded by visual inspection satellite imagery from Google Earth. The top 150 largest cities (rank in GDP/GDP per capita in 2013) in China and

the 47 large US cities selected for analyses in Russell et al. (2012) were also examined. To assure a good fit performance, the following criteria have been defined: (1) The signal of the source is strong, i.e., the mean $NO_2$ TVCD in a circle of 100 km around the location center is larger than $1\times10^{15}$ molec/cm$^2$; and (2) Fit results with poor performance are discarded (see sections 2.2.2 and 2.2.3 for details). The number of wind direction sectors with a good lifetime fit performance is 4 on average. Table S2 of the supplementary material provides a list of all sources under investigation which passed the criteria, including 24 power plants and 69 cities across China and the US.

## 2.6 Impact of topography

The accuracy of fitted lifetimes is highly dependent on the accuracy of the a priori wind directions (used for "sorting" the satellite $NO_2$ observations) and velocities (used for converting $x_0$ into $\tau$). However, accurate modelling of wind fields on small scales is challenging for large-scale models like ECMWF, which do not resolve urban scales. Consequently, wind fields might be biased in particular over complex mountainous terrain, related to the difficulties in resolving the characterization of small-scale orography in models (Beljaars et al., 2004).

We investigate the impact of topography by comparing ECMWF wind fields to 2005–2013 sounding measurements assembled by University of Wyoming (http://weather.uwyo.edu/upperair/sounding.html), and illustrate it for the cities of Harbin (plain terrain) and Taiyuan (mountainous city in Shanxi, China) in Fig. 4. In the top panels, topography used by ECMWF is compared to the topographic data from the 30-arc-sec global land topography "GTOPO30" archived by the U.S. Geological Survey (available at https://lta.cr.usgs.gov/GTOPO30, rescaled to 0.05°). Topographic variations are smeared out significantly by the topographic model used in ECMWF, due to its coarser spatial resolution of 0.36°. The bottom panels show statistics for wind vectors below 500 m during daytime (12:00) and nighttime (0:00) from both ECMWF and the sounding measurements. The frequency distribution of wind

directions (in 45 degree bins) shows a very good agreement in Harbin, but not in Taiyuan: here southerly flows dominate according to sounding measurements, while easterly winds dominate in ECMWF.

We compared wind fields for cities where the fits work properly (Table S2) and the sounding measurements are available simultaneously, as presented in Table S3. For a mountainous city where the elevation in ECMWF contrasted sharply with that in GTOPO, Denver for instance, the correlation in wind speeds between ECMWF and sounding measurements is found to be much lower than for a non-mountainous city like Harbin.

Note that an error in a priori wind direction generally leads to a misclassification during the sorting of the satellite data (see also Sect. 3 of the supplement). In such a case, the assumed wind component in direction of the sector is higher than the actual projection; if, for instance, the true wind would be 5 m/s from north, but the model wind is 5 m/s from east, the case is classified as easterly, while the actual easterly wind is 0. This leads to a systematic high biased projected wind speed in Eq. (4), and thus a low biased lifetime. Thus, mountainous sites often yield very low lifetimes (Table S2).

As the fitted lifetimes, and thus also emissions, rely on appropriate wind fields, we exclude mountainous sites from the following analysis. We simply define a site as mountainous where the absolute difference in elevation between ECMWF and GTOPO is larger than 250 m. A total of seven power plants and 16 cities are rejected based on the criteria, as listed in Table S4. Seven sites in Table S3 fulfill this criteria and 6 of them present low correlation ($r^2$ <0.5) in wind speeds between ECMWF and sounding measurements.

## 3 Results and Discussions

We applied our modified method for determining $NO_x$ lifetimes and emissions to 17 power plants and 53 cities across China and the US (see Fig. 5), which passed the

criteria defined in Sect. 2.5 and Sect.2.6. Some strong cities and power plants are not included as they are mountainous, e.g. Denver or Salt Lake City.

### 3.1 Lifetimes

Figure 6 illustrates the fitted $NO_x$ lifetimes for power plants and cities across China and the US, which demonstrates the wide applicability of the modified method developed in this study. The derived lifetimes in "ozone season" (May-September) are 3.8 ± 1.0 hours (mean ± standard deviation) on average with ranges of 1.8 to 7.5 hours. These values are in agreement to previously reported $NO_x$ lifetimes (e.g., Beirle et al., 2004; Schaub et al., 2007; Beirle et al., 2011; Valin et al., 2013) and correspond to a mean OH concentration of the order of $10^7$ molecules/cm$^3$ (Valin et al., 2013), which is a realistic number for a polluted urban plume around noon (e.g., Kramp and Volz-Thomas, 1997; Dillon et al., 2002; Hofzumahaus et al., 2009). For the investigated sites, average lifetime for Power Plants (3.5 hours) was found to be slightly shorter than for cities (3.9 hours). Individual lifetimes have uncertainties of about 60%. But, still, Fig. 6 indicates that lifetimes are not completely random, but show systematic spatial patterns. We could not unambiguously relate the variability of $NO_x$ lifetime to a driving parameter, like surface elevation, mean wind characteristics, or latitude. But there is a tendency that $NO_x$ lifetime is longer in heavily polluted regions with higher $NO_2$ TVCDs, e.g., eastern China and eastern US: The mean $NO_2$ TVCD for the ozone season in a circle with a radius of 100 km around sources with lifetimes over 5 hours is $6.3\times10^{15}$ molec/cm$^2$, while it is only $1.3\times10^{15}$ molec/cm$^2$ for sources with lifetime less than 2 hours. This finding might be related to nonlinear $NO_x$ chemistry, resulting in a positive correlation between $NO_x$ lifetimes and $NO_2$ TVCDs when the concentration of $NO_x$ is high (Valin et al., 2013). However, we also find that a high $NO_x$ concentration does not necessarily correspond to a long lifetime, and the correlation between $NO_x$ lifetime and $NO_2$ TVCDs is rather low ($r^2$=0.22), probably due to the complex $NO_x$ chemistry, which is as well affected by meteorological and chemical variability, like variations in UV flux, water vapor and VOC levels. In addition, we used tropospheric HCHO columns from OMI (provided by BIRA, De

Smedt et al., 2015) to investigate a potential link between VOCs and the estimated $NO_x$ lifetimes. We averaged the HCHO columns for the ozone season during 2005−2013, and explore their relationship with $NO_x$ lifetime. We observed systematic spatial patterns for the HCHO columns, e.g., the concentration of HCHO is higher in the eastern US than the western US, which is similar to the spatial distribution of $NO_x$ lifetime. However, the overall correlation between HCHO TVCDs and $NO_x$ lifetime is still rather low ($r^2$ = 0.13). Thus, we see no indication that VOCs are the main drivers for the spatial variability of $NO_x$ lifetime.

The proposed method estimates the mean lifetime basically from the change of $NO_2$ patterns for windy vs. calm conditions. Valin et al. (2013) report on a dependency of the $NO_x$ lifetime on wind speed, with generally shorter lifetimes for higher wind speed. In addition, other factors, like the satellite's sensitivity (affected by e.g. cloud properties or the vertical $NO_x$ profile) and the $NO_2$ background might change systematically between calm and windy conditions. In the fitted model function *N(x)*, a scaling factor *a* and an offset *b* are required in order to achieve a good fit performance for the individual fits, which probably compensate for these effects. But on average, the derived values for *a* and *b* are close to 1 and 0, respectively: *a* is 0.9 ± 0.1 (mean ± standard deviation) and *b* is 0.0 ± 0.1×$10^{23}$ molec/cm (mean ± standard deviation).

Thus, possible systematic effects due to all kind of changes between calm and windy conditions are small, and they are considered with a 10% of contribution in the total uncertainty for $NO_x$ lifetimes (see supplement).

We also performed an additional analysis of seasonal mean lifetimes (see supplement, Fig. S4). Wintertime is excluded in the seasonal analysis, because in winter satellite data exhibits larger uncertainties and line densities under calm wind condition are often unrepresentative of the emission pattern due to longer $NO_x$ lifetimes. The seasonal lifetimes reveal higher uncertainties due to a smaller number of available satellite observations compared to the ozone season and thus reduced number of wind direction sectors that yielding a valid fit. The uncertainty is sometimes too large to get

reasonable seasonal patterns for a specific location. But still a systematic seasonal variability can be observed for most non-mountainous cases: mean lifetimes are found to be shorter in summer (3.2 hours) compared to spring (4.2 hours) and autumn (4.5 hours), as expected.

For some locations, the resulting emissions vary considerably over season, which again can be attributed to the poor statistics; in particular spatial gaps can cause high uncertainties of the determined total $NO_2$ mass based on Eq. (5).

## 3.2 Emissions

Figure 7 compares the derived $NO_x$ emissions to bottom-up emission inventories (Sect. 2.4) for all 17 power plants and 53 cities. For power plants, the comparison (Fig. 7a) shows excellent agreement with a high correlation coefficient ($r^2$=0.93). Average emissions are 29 mol/s in bottom-up inventories and 31 mol/s in top-down estimates. The relative difference (defined as $(E_{top\ down} - E_{bottom\text{-}up})/E_{bottom\text{-}up}$) is within 30% for most sites, and 5% ± 27% (mean ± standard deviation) on average. For China and the US, the relative differences are 4% ± 18% and 5% ± 31% respectively, confirming the rather good agreement between CPED/eGRID bottom-up emission inventories and top-down estimates.

For the investigated cities, good agreement (Fig. 7b) between the derived emissions and the bottom-up emissions is reassuring and the $r^2$ reaches 0.84 (0.87 and 0.74 for China and the US respectively). The relative difference between derived $NO_x$ emissions and bottom-up emissions for cities is larger than that for power plants, reaching 9% ± 49% (1% ± 46% and 20% ± 51% for China and the US respectively) on average. This is probably related to the higher uncertainties of the bottom-up inventories for cities compared to those for power plants. Bottom-up emission inventories, developed by different researchers, often differ significantly from each other, due to the application of various assumptions and extrapolations associated with their knowledge of activity data and emission factors. We further compared the representations of China's urban emissions between MEIC and EDGAR, as shown in

Fig. 8. Huge discrepancies are found between EDGAR and top-down estimates (relative difference: 311% ± 412%) with large negative bias in the bottom-up. Considering the deviation in national total $NO_x$ emissions is far less (20.7 and 24.9 Tg-$NO_2$ for year 2008 in EDGAR and MEIC respectively), the large bias could be primarily explained by the spatial distributions in the two inventories.

Both MEIC and EDGAR calculate emissions as province/country totals and distribute them to grids using spatial proxies. By comparing spatial proxies used in the two inventories, we identified the major differences in spatial allocation methods between them: (1) MEIC used an in-house high-resolution database (CPED) to represent power plant emissions in China while EDGAR used CARMA (Wheeler and Ummel, 2008). The coordinates of power plants in CARMA are highly uncertain for China (Liu et al., 2015); (2) for industrial emissions, MEIC first downscaled provincial totals to counties using industrial GDP, and then allocate county emissions to grids with population density. EDGAR directly distributed provincial emissions by population density (EC-JRC/PBL, 2012); and (3) MEIC allocated on-road emissions by vehicle and road type using the China Digital Road-network Map (Zheng et al., 2014), while EDGAR used the product of population density (Gridded Population of the World (GPW) version 3, (CIESIN et al., 2005)) and road network (the Global Roads Inventory Project (GRIP), (PBL, 2008)). All above factors are expected to contribute to the better representations of urban emissions in MEIC than in EDGAR over China, and thus gain better agreement with top-down estimates.

It is interesting that EDGAR represents urban emissions much better in the US than in China, even though EDGAR shared the same spatial allocation approach across different countries. One plausible explanation is that spatial proxies work better in the US, implying the linear relationships between emissions and proxies, e.g., vehicle emissions and road densities, industrial/residential emissions and population densities. Different accuracy of spatial proxies among regions may also contribute to the discrepancy of performance in the two inventories. For instance, the GRIP database (http://geoservice.pbl.nl/website/GRIP/) missed too many roads for China (Fig. S6).

By comparing with a high-resolution emission inventory, the Database of Road Transportation Emissions (DARTE), Gately et al. (2015) argued that EDGAR overestimated on-road emissions in city centers while underestimate at the suburban and exurban fringes, resulting from mismatches between road density and the actual spatial patterns of vehicle activity at urban scales. To better understand the uncertainties associated with the performance of spatial proxies, further source-by-source comparison is required between downscaled regional inventories and high-resolution inventories independent to spatial proxies (e.g., DARTE).

The emissions are derived based on the individual fitted lifetimes for each site. If, instead, the mean lifetime of all sites (3.7 hours) would be considered for the calculation of emissions, the correlations to bottom-up emissions are worse compared to the individual fitted $NO_x$ lifetime (Fig. 9). This holds for both, power plants and cities. We conclude that variation of the fitted lifetime is not just the result of statistical noise, but actually carries information on local variability of the oxidizing capacity of urban plumes. The individual lifetimes are thus well suited for the determination of emissions by a mass balance approach.

Satellite observations also enable the study of spatial and temporal distributions of $SO_2$ emissions (e.g., Fioletov et al. (2011)) and even to obtain estimates of $SO_2$ lifetimes and emissions under special circumstances (e.g., Beirle et al. (2014)). However, if the method developed in this study would be applied to $SO_2$ directly, higher uncertainties have to be expected due to the longer lifetime of $SO_2$ (see Sect. 5 of the supplement for a detailed discussion).

### 3.3 Uncertainties

Based on the approaches presented in Sect. 3 of the supplement, we estimated that total uncertainties of $NO_x$ lifetime and emissions are within 39%–80% and 55%–91% respectively for all the investigated sites (see Sect. 2.5). For Harbin, relative uncertainties for mean lifetime and emissions are 43% and 58%, respectively. However, it is worth noting that our uncertainty estimate is rather conservative. For

power plants, relative differences between bottom-up and top-down estimates are all within 50% (Fig. 7a). As bottom-up emission inventories for power plants are well developed with low uncertainties, the good consistency increases our confidence that the fitted emissions well represent the real-word emission characteristic. Thus, bottom-up inventories may have large biases for cities where emission estimates differ significantly from top-down constraints (i.e., the relative difference far exceeds 50%).

From the quantitative analysis approach described in Sect.2.3, we identify the uncertainties induced by individual factors. Detailed discussions are presented in the supplementary information. In summary, we conclude that

- the uncertainty due to wind data is ~30% (affecting both $\tau$ and emissions),
- effects of a possible systematic change of $NO_2$ TVCDs from calm (used for fit of $E$) to windy (used for fit of $\tau$) conditions are small (<10%),
- the derived emissions (but not the lifetimes) are affected by the uncertainty of the $NO_2$ TVCDs (~30%) and the $NO_x/NO_2$ scaling factor (~10%),
- the dependency on the definition of integration and fit intervals is about 10%,
- the CI of fitted lifetimes and total $NO_2$ mass is about 30% and 20%, respectively; the standard mean error of fitted lifetimes for different wind directions is less than 40% (see Sect.3 of supplement).

All involved uncertainties contain both statistical fluctuations as well as systematic effects. By ongoing satellite measurements (e.g. TROPOMI), i.e. longer available time periods, and the much better temporal sampling of upcoming geostationary satellite missions such as GEMS (Kim et al., 2012), TEMPO (Chance et al., 2012), or Sentinel-4 (Ingmann et al., 2012), statistical uncertainties will decrease. In addition, we expect further improvement of the presented lifetime fit method by using regional meteorological models that are more capable of representing wind fields in the planetary boundary layer especially for mountainous region. Also the uncertainties of TVCDs from satellite retrievals, which is still the largest single component of total

uncertainty in top-down emission estimates, is expected to decrease in the coming years: input data such as surface albedo or a priori profiles will improve, and the current intensive validation efforts (e.g., DISCOVER-AQ (http://discover-aq.larc.nasa.gov/) and AROMAT (http://uv-vis.aeronomie.be/aromat/)) will help to identify and remove systematic errors. It can thus be expected that total uncertainties of the proposed method will decrease significantly within the next decade.

## 4 Conclusion

We developed a new method to estimate $NO_x$ lifetimes and emissions of power plants and cities in polluted background from satellite $NO_2$ observations. The method improves upon that of Beirle et al. (2011) by explicitly accounting for interferences with neighboring strong $NO_x$ sources by using $NO_2$ spatial patterns under calm wind conditions as proxy of the patterns of emission sources. Lifetimes are derived from the change of $NO_2$ distributions under windy compared to calm conditions. $NO_x$ emissions are derived by mass balance: the total mass of $NO_2$ originating from the source of interest is divided by the lifetime derived for the corresponding source.

The new method for determining $NO_x$ lifetimes and emissions was applicable for 24 power plants and 69 cities over China and the US, including 23 mountainous sites. We exclude the derived results for 23 mountainous sites from the analysis, which are expected to have larger uncertainties owing to the inaccurate wind data. The derived lifetimes for 70 non-mountainous sites are 3.8 ± 1.0 hours (mean ± standard deviation) on average with ranges of 1.8 to 7.5 hours. We observed systematic spatial patterns for the derived lifetimes, which however could not be simply explained by a specific driving parameter. Generally, higher lifetimes were found in heavily polluted regions, but the overall correlation between $NO_2$ TVCDs and $NO_x$ lifetime is quite low ($r^2$= 0.22).

The derived top-down $NO_x$ emissions are generally in very good agreement with bottom-up emission inventories, in particular for power plants, while correlations for cities were lower, probably due to the higher uncertainty of the bottom-up inventories

for cities. Compared to MEIC, the EDGAR global inventory significantly underestimated $NO_x$ emissions for Chinese cities, because spatial proxies used in EDGAR may misrepresent emission spatial patterns for China.

Owing to the global continuous monitoring of satellite measurements, this method can be applied to quantify the emissions from various cities and power plants even in polluted background around the world. For this study, we choose large sources across China and the US as the pre-selected candidates, of which the good-quality bottom-up emission information, particularly for power plants, is available. Further investigation on sources located in other regions, in particular, Europe, will be performed in the near future, with collating the corresponding bottom-up emission inventories. This capability will further be enhanced with future satellite instrument like TROPOMI (Veefkind et al., 2012) featuring higher spatial resolution. In addition, upcoming geostationary satellite instruments will enable studies on the diurnal cycle of the $NO_x$ lifetime. More accurate estimates for emission rates, trends and seasonality can be expected, which will serve as an independent data source to validate bottom-up emission estimates in the future.

## Acknowledgements

This work was funded by the National Natural Science Foundation of China (41222036, 41275026, 41571130032), the China's National Basic Research Program (2014CB441301), and the EU FP-7 Program MarcoPolo (606953). F. Liu acknowledges the financial support from China Scholarship Council. Q. Zhang and K. B. He are supported by the Collaborative Innovation Center for Regional Environmental Quality. We acknowledge the free use of tropospheric $NO_2$ TVCDs (DOMINO v2.0) from the OMI sensor from www.temis.nl. We thank the ECMWF for providing wind fields, the US Geological Survey for providing GTOPO30, and the University of Wyoming for providing sounding measurements. We thank the four anonymous reviewers for helpful comments during ACP discussions.

## References

Beirle, S., Platt, U., Wenig, M., and Wagner, T.: Weekly cycle of $NO_2$ by GOME measurements: A signature of anthropogenic sources, Atmos. Chem. Phys., 3, 2225–2232, doi:10.5194/acp-3-2225-2003, 2003.

Beirle, S., Platt, U., von Glasow, R., Wenig, M., and Wagner, T.: Estimate of nitrogen oxide emissions from shipping by satellite remote sensing, Geophys. Res. Lett., 31, L18102, doi:10.1029/2004GL020312, 2004.

Beirle, S., Boersma, K. F., Platt, U., Lawrence, M. G., and Wagner, T.: Megacity emissions and lifetimes of nitrogen oxides probed from space, Science, 333, 1737–1739, 2011.

Beirle, S., Hörmann, C., Penning de Vries, M., Dörner, S., Kern, C., and Wagner, T.: Estimating the volcanic emission rate and atmospheric lifetime of $SO_2$ from space: a case study for Kīlauea volcano, Hawai'i, Atmos. Chem. Phys., 14, 8309–8322, doi:10.5194/acp-14-8309-2014, 2014.

Beljaars, A. C. M., Brown, A. R., and Wood, N.: A new parametrization of turbulent orographic form drag, Quarterly Journal of the Royal Meteorological Society, 130, 1327–1347, 2004.

Boersma, K. F., Eskes, H. J., Dirksen, R. J., van der A, R. J., Veefkind, J. P., Stammes, P., Huijnen, V., Kleipool, Q. L., Sneep, M., Claas, J., Leitão, J., Richter, A., Zhou, Y., and Brunner, D.: An improved tropospheric $NO_2$ column retrieval algorithm for the Ozone Monitoring Instrument, Atmos. Meas. Tech., 4, 1905–1928, doi:10.5194/amt-4-1905-2011, 2011.

Butler, T. M., Lawrence, M. G., Gurjar, B. R., van Aardenne, J., Schultz, M., and Lelieveld, J.: The representation of emissions from megacities in global emission inventories, Atmos. Environ., 42, 703–719, 2008.

Celarier, E. A., Brinksma, E. J., Gleason, J. F., Veefkind, J. P., Cede, A., Herman, J. R., Ionov, D., Goutail, F., Pommereau, J. P., Lambert, J. C., van Roozendael, M., Pinardi, G., Wittrock, F., Schönhardt, A., Richter, A., Ibrahim, O. W., Wagner, T., Bojkov, B., Mount, G., Spinei, E., Chen, C. M., Pongetti, T. J., Sander, S. P., Bucsela, E. J., Wenig, M. O., Swart, D. P. J., Volten, H., Kroon, M., and Levelt, P. F.: Validation of Ozone Monitoring Instrument nitrogen dioxide columns, J. Geophys. Res., 113, D15S15, doi:10.1029/2007JD008908, 2008.

Center for International Earth Science Information Network (CIESIN), Food and Agriculture Organization of the United Nations (FAO), and Centro Internacional de Agricultura Tropical (CIAT): Gridded Population of the World, version 3 (GPWv3): Population Count Grid, available at: http://sedac.ciesin.columbia.edu/data/set/gpw-v3-population-count (last accessed: 10 June, 2015), 2005.

Chance, K., Lui, X., Suleiman, R. M., Flittner, D. E., and Janz, S.J.: Tropspheric Emissions: Monitoring of Pollution (TEMPO), presented at the 2012 AGU Fall Meeting, San Francisco, USA, 3–7 December 2012, A31B-0020, 2012.

de Foy, B., Wilkins, J. L., Lu, Z., Streets, D. G., and Duncan, B. N.: Model evaluation of methods for estimating surface emissions and chemical lifetimes from satellite data, Atmos. Environ., 98, 66–77, 2014.

de Foy, B., Lu, Z., Streets, D. G., Lamsal, L. N., and Duncan, B. N.: Estimates of power plant $NO_x$ emissions and lifetimes from OMI $NO_2$ satellite retrievals, Atmos. Environ., 116, 1–11, 2015.

Dee, D. P., Uppala, S. M., Simmons, A. J., Berrisford, P., Poli, P., Kobayashi, S., Andrae, U., Balmaseda, M. A., Balsamo, G., Bauer, P., Bechtold, P., Beljaars, A. C. M., van de Berg, L., Bidlot, J., Bormann, N., Delsol, C., Dragani, R., Fuentes, M., Geer, A. J., Haimberger, L., Healy, S. B., Hersbach, H., Hólm, E. V., Isaksen, L., Kållberg, P., Köhler, M., Matricardi, M., McNally, A. P., Monge-Sanz, B. M., Morcrette, J. J., Park, B. K., Peubey, C., de Rosnay, P., Tavolato, C., Thépaut, J. N., and Vitart, F.: The ERA-Interim reanalysis: configuration and performance of the data assimilation system, Quarterly Journal of the Royal Meteorological Society, 137, 553–597, 2011.

De Smedt, I., Stavrakou, T., Hendrick, F., Danckaert, T., Vlemmix, T., Pinardi, G., Theys, N., Lerot, C., Gielen, C., Vigouroux, C., Hermans, C., Fayt, C., Veefkind, P., Müller, J. F., and Van Roozendael, M.: Diurnal, seasonal and long-term variations of global formaldehyde columns inferred from combined OMI and GOME-2 observations, Atmos. Chem. Phys., 15, 12519–12545, doi:10.5194/acp-15-12519-2015, 2015.

Dillon, M. B., Lamanna, M. S., Schade, G. W., Goldstein, A. H., and Cohen, R. C.: Chemical evolution of the Sacramento urban plume: Transport and oxidation, J. Geophys. Res., 107, D5, doi:10.1029/2001JD000969, 2002.

Ding, J., van der A, R. J., Mijling, B., Levelt, P. F., and Hao, N.: $NO_x$ emission estimates during the 2014 Youth Olympic Games in Nanjing, Atmos. Chem. Phys., 15, 9399–9412, doi:10.5194/acp-15-9399-2015, 2015.

Duncan, B. N., Yoshida, Y., de Foy, B., Lamsal, L. N., Streets, D. G., Lu, Z., Pickering, K. E., and Krotkov, N. A.: The observed response of Ozone Monitoring Instrument (OMI) $NO_2$ columns to $NO_x$ emission controls on power plants in the United States: 2005–2011, Atmos. Environ., 81, 102–111, 2013.

European Commission (EC): Joint Research Centre (JRC)/Netherlands Environmental Assessment Agency (PBL), Emission Database for Global Atmospheric Research (EDGAR), release version 4.2, available at: http://edgar.jrc.ec.europa.eu (last access: 1 December 2013), 2011.

European Commission (EC): Joint Research Centre (JRC)/Netherlands Environmental Assessment Agency (PBL), Global emission inventories in the Emission Database for Global Atmospheric Research (EDGAR) – Manual (I) Gridding: EDGAR emissions distribution on global gridmaps, available at: http://publications.jrc.ec.europa.eu/repository/bitstream/JRC78261/edgarv4_manual_i_gridding_pubsy_final.pdf (last accessed: 1 June, 2015), 2012.

Fioletov, V. E., McLinden, C. A., Krotkov, N., Moran, M. D., and Yang, K.: Estimation of $SO_2$ emissions using OMI retrievals, Geophys. Res. Lett., 38, L21811, doi:10.1029/2011gl049402, 2011.

Fioletov, V. E., McLinden, C. A., Krotkov, N., and Li, C.: Lifetimes and emissions of $SO_2$ from point sources estimated from OMI, Geophys. Res. Lett., 42, 2015GL063148, doi:10.1002/2015gl063148, 2015.

Gately, C. K., Hutyra, L. R., and Sue Wing, I.: Cities, traffic, and $CO_2$: A multidecadal assessment of trends, drivers, and scaling relationships, Proceedings of the National Academy of Sciences, 112, 4999–5004, 2015.

Gluck, S., Glenn, C., Logan, T., Vu, B., Walsh, M., and Williams, P.: Evaluation of $NO_x$ flue gas analyzers for accuracy and their applicability for low-concentration measurements, J. Air Waste Manage. Assoc., 53, 749758, 2003.

Gu, D., Wang, Y., Smeltzer, C., and Liu, Z.: Reduction in $NO_x$ emission trends over China: Regional and seasonal variations, Environ. Sci. Technol., 47, 12912–12919, 2013.

Hilboll, A., Richter, A., and Burrows, J. P.: Long-term changes of tropospheric $NO_2$ over megacities derived from multiple satellite instruments, Atmos. Chem. Phys., 13, 4145–4169, doi:10.5194/acp-13-4145-2013, 2013.

Hofzumahaus, A., Rohrer, F., Lu, K., Bohn, B., Brauers, T., Chang, C.-C., Fuchs, H., Holland, F., Kita, K., Kondo, Y., Li, X., Lou, S., Shao, M., Zeng, L., Wahner, A., and Zhang, Y.: Amplified Trace Gas Removal in the Troposphere, Science, 324, 1702–1704, 2009.

Ingmann, P., Veihelmann, B., Langen, J., Lamarre, D., Stark, H., and Courrèges-Lacoste, G. B.: Requirements for the GMES Atmosphere Service and ESA's implementation concept: Sentinels-4/-5 and-5p, Remote Sens. Environ., 120, 58–69, 2012.

Jacob, D. J., Heikes, E. G., Fan, S. M., Logan, J. A., Mauzerall, D. L., Bradshaw, J. D., Singh, H. B., Gregory, G. L., Talbot, R. W., Blake, D. R., and Sachse, G. W.: Origin of ozone and $NO_x$ in the tropical troposphere: A photochemical analysis of aircraft observations over the South Atlantic basin, J. Geophys. Res., 101, 24235–24250, doi:10.1029/96jd00336, 1996.

Kim, S. W., Heckel, A., Frost, G. J., Richter, A., Gleason, J., Burrows, J. P., McKeen, S., Hsie, E. Y., Granier, C., and Trainer, M.: $NO_2$ columns in the western United States observed from space and simulated by a regional chemistry model and their implications for $NO_x$ emissions, J. Geophys. Res., 114, D11301, doi:10.1029/2008jd011343, 2009.

Kim, J.: GEMS (Geostationary Enviroment Monitoring Spectrometer) onboard the GeoKOMPSAT to monitor air quality in high temporal and spatial resolution over Asia-Pacific region, presented at the 2012 EGU General Assembly, Vienna, Austria, 22–27 April 2012, EGU2012-4051, 2012.

Konovalov, I. B., Beekmann, M., Richter, A., and Burrows, J. P.: Inverse modelling of the spatial distribution of $NO_x$ emissions on a continental scale using satellite data, Atmos. Chem. Phys., 6, 1747–1770, doi:10.5194/acp-6-1747-2006, 2006.

Kramp, F., and Volz-Thomas, A.: On the Budget of OH Radicals and Ozone in an Urban Plume from the Decay of C5–C8 Hydrocarbons and $NO_x$, Journal of Atmospheric Chemistry, 28, 263–282, 1997.

Lamsal, L. N., Martin, R. V., Padmanabhan, A., van Donkelaar, A., Zhang, Q., Sioris, C. E., Chance, K., Kurosu, T. P., and Newchurch, M. J.: Application of satellite observations for timely updates to global anthropogenic $NO_x$ emission inventories, Geophys. Res. Lett., 38, L05810, doi:10.1029/2010gl046476, 2011.

Lelieveld, J., Beirle, S., Hörmann, C., Stenchikov, G. and Wagner, T.: Abrupt recent trend changes in atmospheric nitrogen dioxide over the Middle East, Science Advances, 1(7), e1500498, doi:10.1126/sciadv.1500498, 2015.

Leue, C., Wenig, M., Wagner, T., Klimm, O., Platt, U., and Jähne, B.: Quantitative analysis of $NO_x$ emissions from Global Ozone Monitoring Experiment satellite image sequences, J. Geophys. Res., 106, 5493–5505, doi:10.1029/2000JD900572, 2001.

Levelt, P. F., van den Oord, G. H. J., Dobber, M. R., Malkki, A., Huib, V., Johan de, V., Stammes, P., Lundell, J. O. V., and Saari, H.: The ozone monitoring instrument, Geoscience and Remote Sensing, IEEE Transactions on, 44, 1093–1101, 2006.

Lin, J. T., Liu, Z., Zhang, Q., Liu, H., Mao, J., and Zhuang, G.: Modeling uncertainties for tropospheric nitrogen dioxide columns affecting satellite-based inverse modeling of nitrogen oxides emissions, Atmos. Chem. Phys., 12, 12255–12275, doi:10.5194/acp-12-12255-2012, 2012.

Liu, F., Zhang, Q., Tong, D., Zheng, B., Li, M., Huo, H., and He, K. B.: High-resolution inventory of technologies, activities, and emissions of coal-fired power plants in China from 1990 to 2010, Atmos. Chem. Phys., 15, 13299–13317, doi:10.5194/acp-15-13299-2015, 2015.

Lu, Z., Streets, D. G., de Foy, B., Lamsal, L. N., Duncan, B. N., and Xing, J.: Emissions of nitrogen oxides from US urban areas: estimation from Ozone Monitoring Instrument retrievals for 2005–2014, Atmos. Chem. Phys., 15, 10367-10383, doi:10.5194/acp-15-10367-2015, 2015.

Martin, R. V., Jacob, D. J., Chance, K., Kurosu, T. P., Palmer, P. I., and Evans, M. J.: Global inventory of nitrogen oxide emissions constrained by space-based observations of $NO_2$ columns, J. Geophys. Res., 108, 4537, doi:10.1029/2003jd003453, 2003.

Martin, R. V., Sioris, C. E., Chance, K., Ryerson, T. B., Bertram, T. H., Wooldridge, P. J., Cohen, R. C., Neuman, J. A., Swanson, A., and Flocke, F. M.: Evaluation of space-based constraints on global nitrogen oxide emissions with regional aircraft measurements over and downwind of eastern North America, J. Geophys. Res., 111, D15308, doi:10.1029/2005JD006680, 2006.

Netherlands Environmental Assessment Agency (PBL), Global Roads Inventory Project (GRIP) database, avalable at: http://geoservice.pbl.nl/website/GRIP/ (last accessed: 15 June, 2015), 2008.

Olivier, J., Peters, J., Bakker, J., Berdowski, J., Visschedijk, A., and Bloos, J.: Applications of EDGAR. Including a description of EDGAR 3.2. Reference database with trend data for 1970–1995, Rijksinstituut voor Volksgezondheid en Milieu RIVM, Bilthoven (Netherlands), 2002.

Platt, U.: Differential optical absorption spectroscopy (DOAS) in: Air monitoring by spectroscopic techniques, edited by: Sigrist, M. W., John Wiley and Sons, New York, 27–76, 1994.

Richter, A., Burrows, J. P., Nusz, H., Granier, C., and Niemeier, U.: Increase in tropospheric nitrogen dioxide over China observed from space, Nature, 437, 129–132, 2005.

Russell, A. R., Valin, L. C., Bucsela, E. J., Wenig, M. O., and Cohen, R. C.: Space-based constraints on spatial and temporal patterns of $NO_x$ emissions in California, 2005–2008, Environ. Sci. Technol., 44, 3608–3615, 2010.

Russell, A. R., Valin, L. C., and Cohen, R. C.: Trends in OMI $NO_2$ observations over the United States: effects of emission control technology and the economic recession, Atmos. Chem. Phys., 12, 12197–12209, doi:10.5194/acp-12-12197-2012, 2012.

Schaub, D., Brunner, D., Boersma, K. F., Keller, J., Folini, D., Buchmann, B., Berresheim, H., and Staehelin, J.: SCIAMACHY tropospheric $NO_2$ over Switzerland: estimates of $NO_x$ lifetimes and impact of the complex Alpine topography on the retrieval, Atmos. Chem. Phys., 7, 5971–5987, doi:10.5194/acp-7-5971-2007, 2007.

Schneider, P., and van der A, R. J.: A global single-sensor analysis of 2002–2011 tropospheric nitrogen dioxide trends observed from space, J. Geophys. Res., 117, D16309, doi:10.1029/2012jd017571, 2012.

Seinfeld, J. H., and Pandis, S. N.: Atmospheric chemistry and physics: From air pollution to climate change, John Wiley and Sons, New York, 204–275, 2006.

USEPA: Technical support document for the 9th edition of eGRID with year 2010 data (the Emissions & Generation Resource Integrated Database), Washington, D.C., 2014.

Valin, L. C., Russell, A. R., and Cohen, R. C.: Variations of OH radical in an urban plume inferred from $NO_2$ column measurements, Geophys. Res. Lett., 40, 1856–1860, doi:10.1002/grl.50267, 2013.

Valin, L. C., Russell, A. R., and Cohen, R. C.: Chemical feedback effects on the spatial patterns of the $NO_x$ weekend effect: a sensitivity analysis, Atmos. Chem. Phys., 14, 1–9, doi:10.5194/acp-14-1-2014, 2014.

Veefkind, J. P., Aben, I., McMullan, K., Förster, H., de Vries, J., Otter, G., Claas, J., Eskes, H. J., de Haan, J. F., Kleipool, Q., van Weele, M., Hasekamp, O., Hoogeveen, R., Landgraf, J., Snel, R., Tol, P., Ingmann, P., Voors, R., Kruizinga, B., Vink, R., Visser, H., and Levelt, P. F.: TROPOMI on the ESA Sentinel-5 Precursor: A GMES mission for global observations of the atmospheric composition for climate, air quality and ozone layer applications, Remote Sens. Environ., 120, 70–83, 2012.

Wheeler, D., and Ummel, K.: Calculating CARMA: Global estimation of $CO_2$ emissions from the power sector, Working Paper 145, Center for Global Development, Washington, D.C., 2008.

Zhang, Q., Streets, D. G., He, K., Wang, Y., Richter, A., Burrows, J. P., Uno, I., Jang, C. J., Chen, D., Yao, Z., and Lei, Y.: $NO_x$ emission trends for China, 1995–2004: The view from the ground and the view from space, J. Geophys. Res., 112, D22306, doi:10.1029/2007jd008684, 2007.

Zhao, Y., Wang, S., Duan, L., Lei, Y., Cao, P., and Hao, J.: Primary air pollutant emissions of coal-fired power plants in China: Current status and future prediction, Atmos. Environ., 42, 8442–8452, 2008.

Zhao, Y., Nielsen, C. P., Lei, Y., McElroy, M. B., and Hao, J.: Quantifying the uncertainties of a bottom-up emission inventory of anthropogenic atmospheric pollutants in China, Atmos. Chem. Phys., 11, 2295–2308, doi:10.5194/acp-11-2295-2011, 2011.

Zheng, B., Huo, H., Zhang, Q., Yao, Z. L., Wang, X. T., Yang, X. F., Liu, H., and He, K. B.: High-resolution mapping of vehicle emissions in China in 2008, Atmos. Chem. Phys., 14, 9787–9805, doi:10.5194/acp-14-9787-2014, 2014.

## Tables

Table 1. Intervals chosen for the fit of the $NO_x$ lifetime and total mass.

| Category | Interval (km) | |
|---|---|---|
| | Wind direction (fit) | Across-wind direction (integration) |
| Fit lifetime | *f* | *i* |
| | 600 | 300 |
| Fit total mass | *h* | *v* |
| Power plant | 100 | 40 |
| City | 200 | 40 |
| Pearl River Delta | 300 | 60 |

# Figures

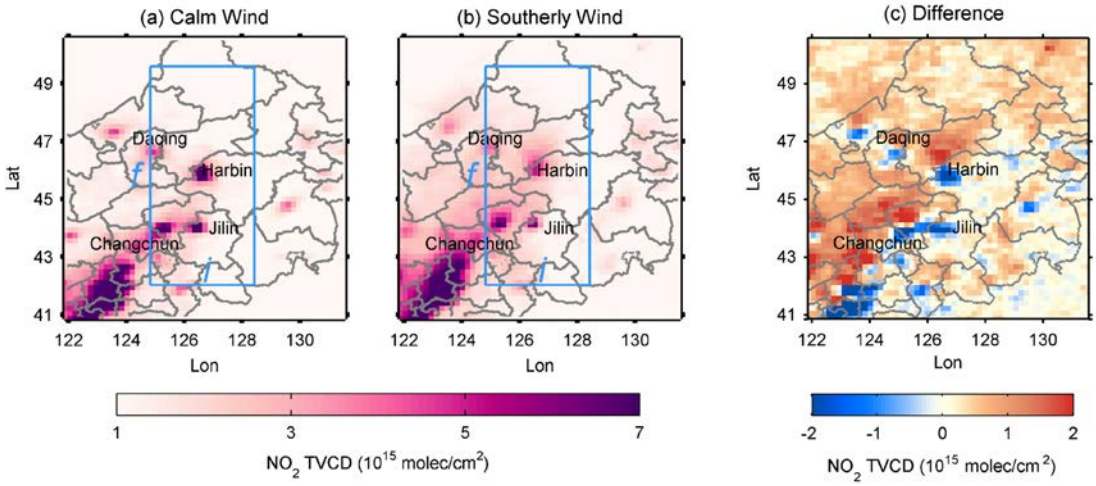


Figure 1. Mean $NO_2$ TVCDs around Harbin for (a) calm, (b) southerly wind conditions and (c) their difference (southerly − calm). For the fit of lifetimes, the mean $NO_2$ TVCDs are integrated over interval *i* in across-wind direction to calculate line densities and the fit is performed over the fit interval *f* (blue lines in (a) and (b); see Sect. 2.2.2 for details).

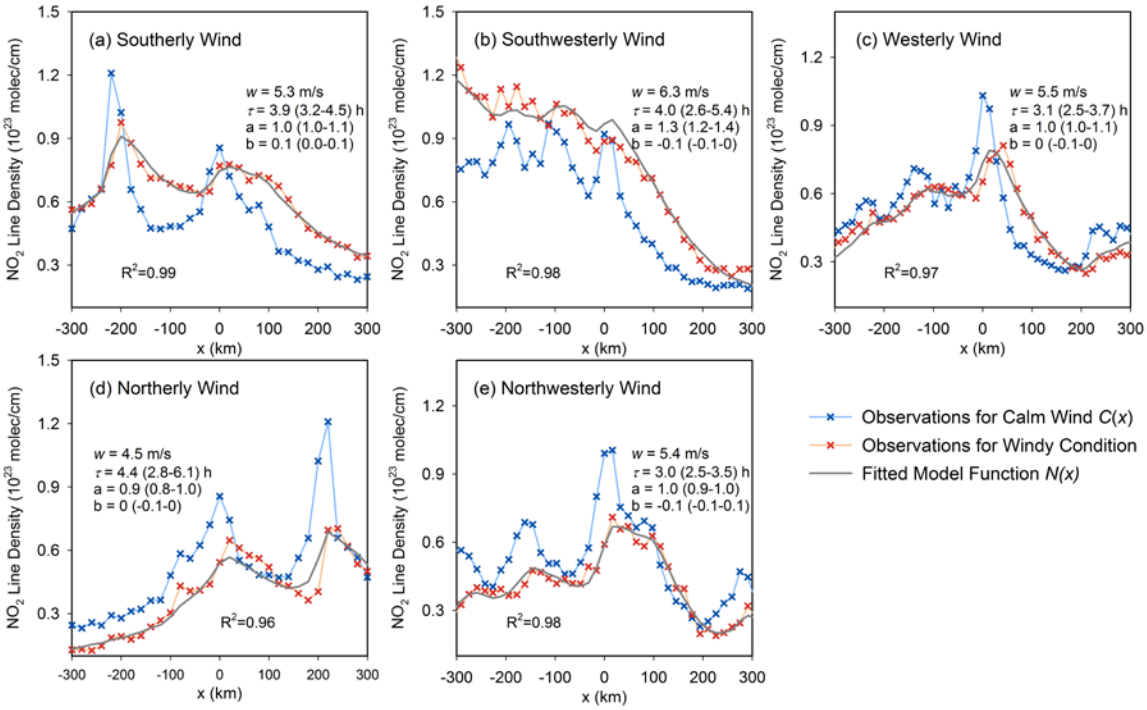


Figure 2. $NO_2$ line densities around Harbin for different wind direction sectors. Crosses: $NO_2$ line densities for calm (blue) and (a) southerly, (b) southwesterly, (c) westerly, (d) northerly and (e) northwesterly (red) winds as function of the distance $x$ to Harbin center. Grey line: the fit result $N(x)$. The numbers indicate the net mean wind velocities (windy − calm) from ECMWF ($w$), the lifetime $\tau$, the factor $a$ and offset $b$ resulting from the least-squares fit with 95% confidence interval. $NO_2$ line densities for the remaining wind direction sectors are dismissed due to missing data (see the criteria of "reliability" defined in Sect. 2.2.2).

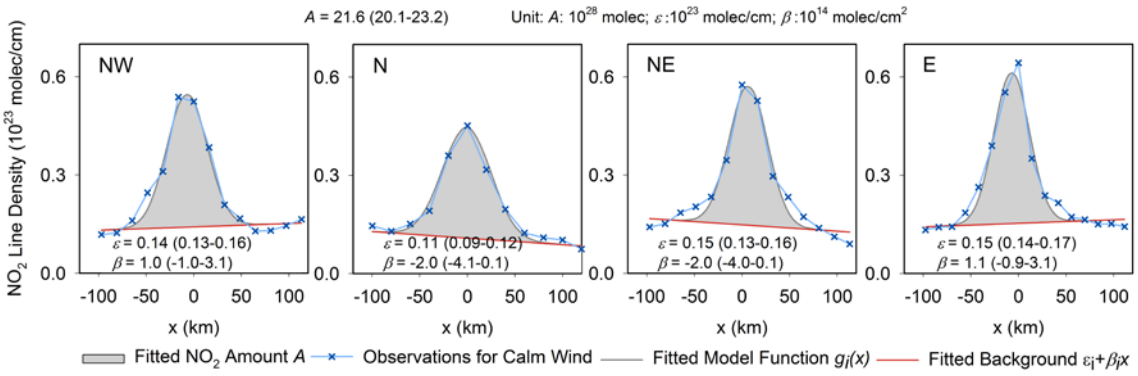


Figure 3. $NO_2$ line densities in Harbin for northwest, north, northeast and east directions (from left to right). Crosses: $NO_2$ line densities for calm winds as function of the distance to Harbin center $x$. Grey line: the fit result $g_i(x)$. Pink line: the fitted background $\varepsilon_i + \beta_i x$. Grey shade: the magnitude of the fitted $NO_2$ amount $A$. The number indicates $A$, the offset $\varepsilon$ and the linear gradient in the background field $\beta$ resulting from the least-squares fit with 95% CI.

(a) Harbin

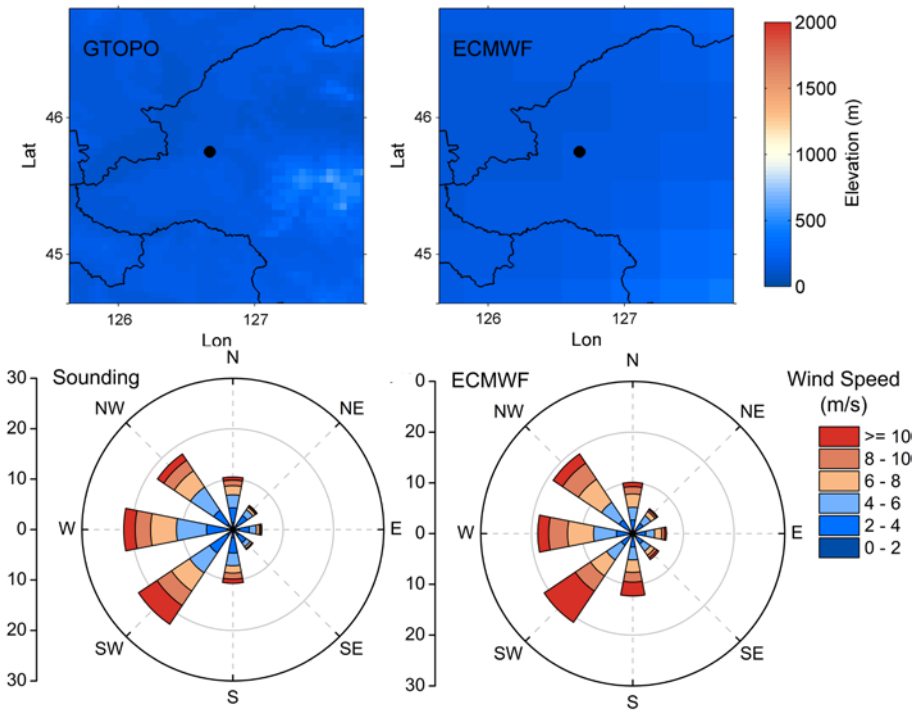


(b) Taiyuan

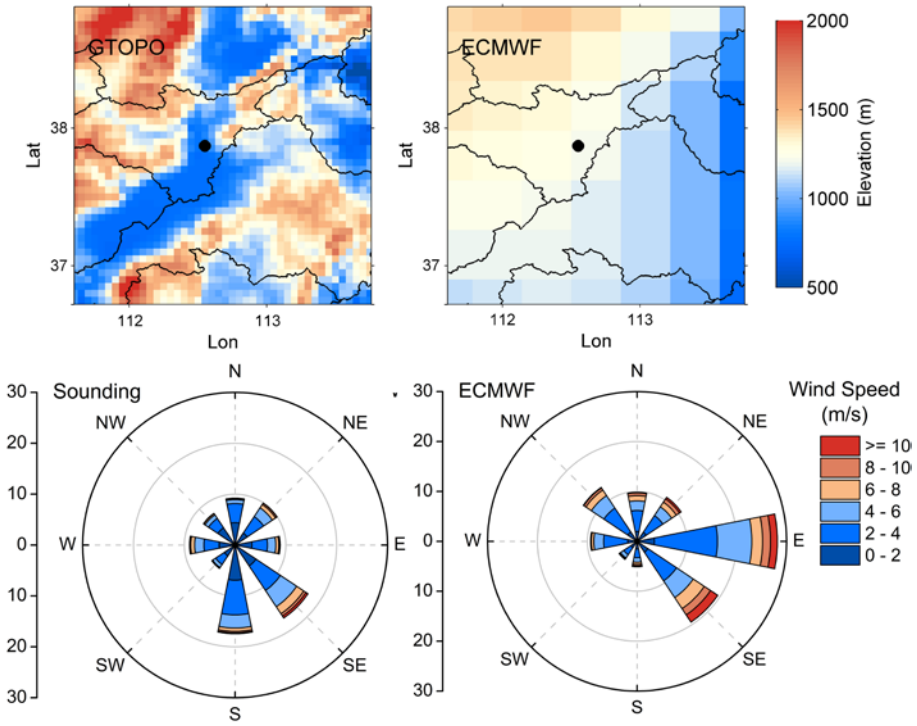


Figure 4. Comparison of the topography (top panel) and wind roses (bottom panel) from ECMWF (right panel) and higher resolution data sets (left panel) around (a) Harbin and (b) Taiyuan. The land surface elevation on the left panel is derived from GTOPO30. The wind roses on the left panel are generated from sounding measurements assembled by University of Wyoming. Radial units are percent per 45°direction band.

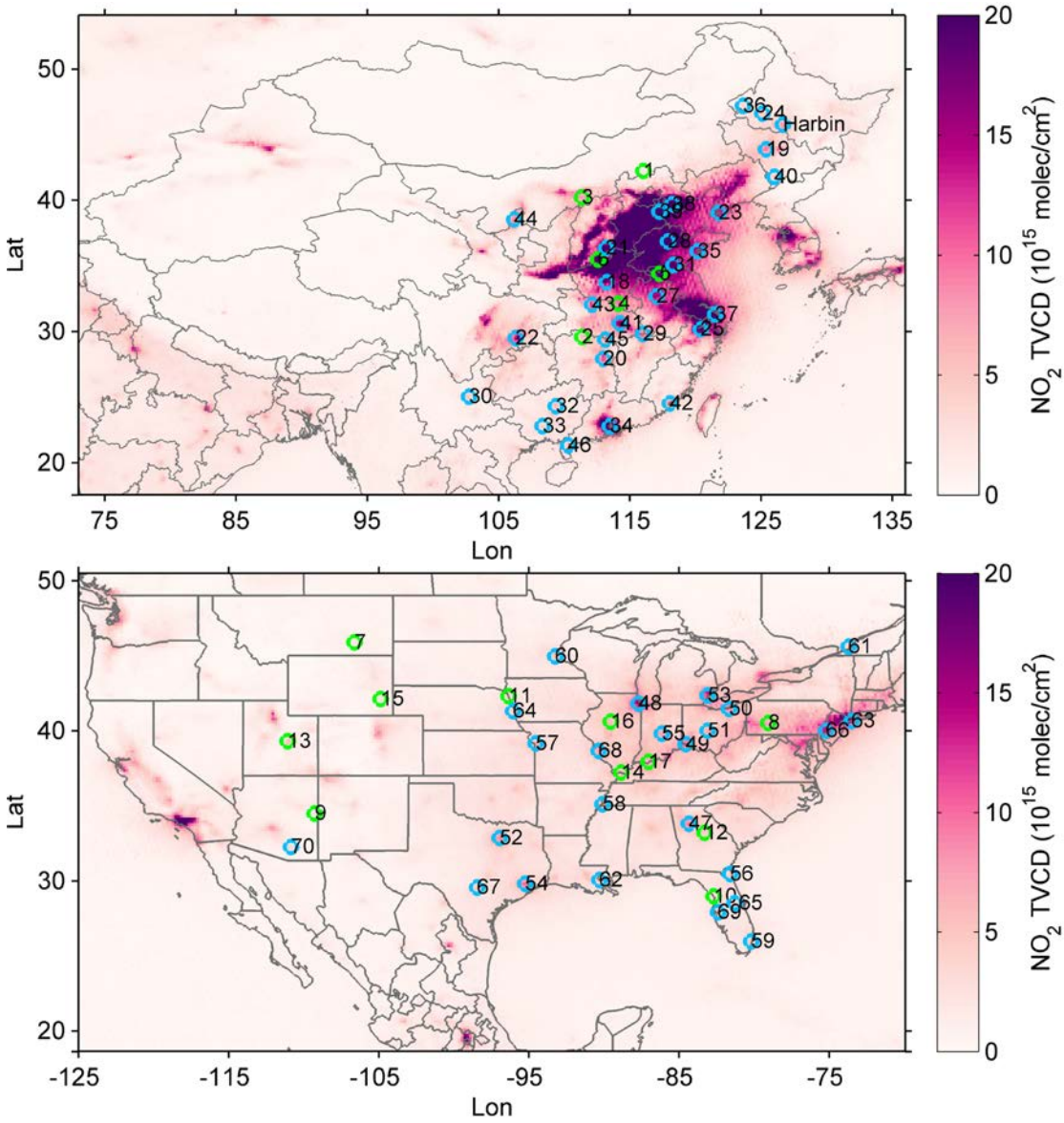


Figure 5. Average OMI $NO_2$ TVCDs during ozone season (i.e., May to September) over China and the US for the period 2005–2013. Green and blue symbols indicate the 17 power plants and 53 cities investigated in this work, respectively. Power plants and cities are labelled by their IDs (see Table S2).

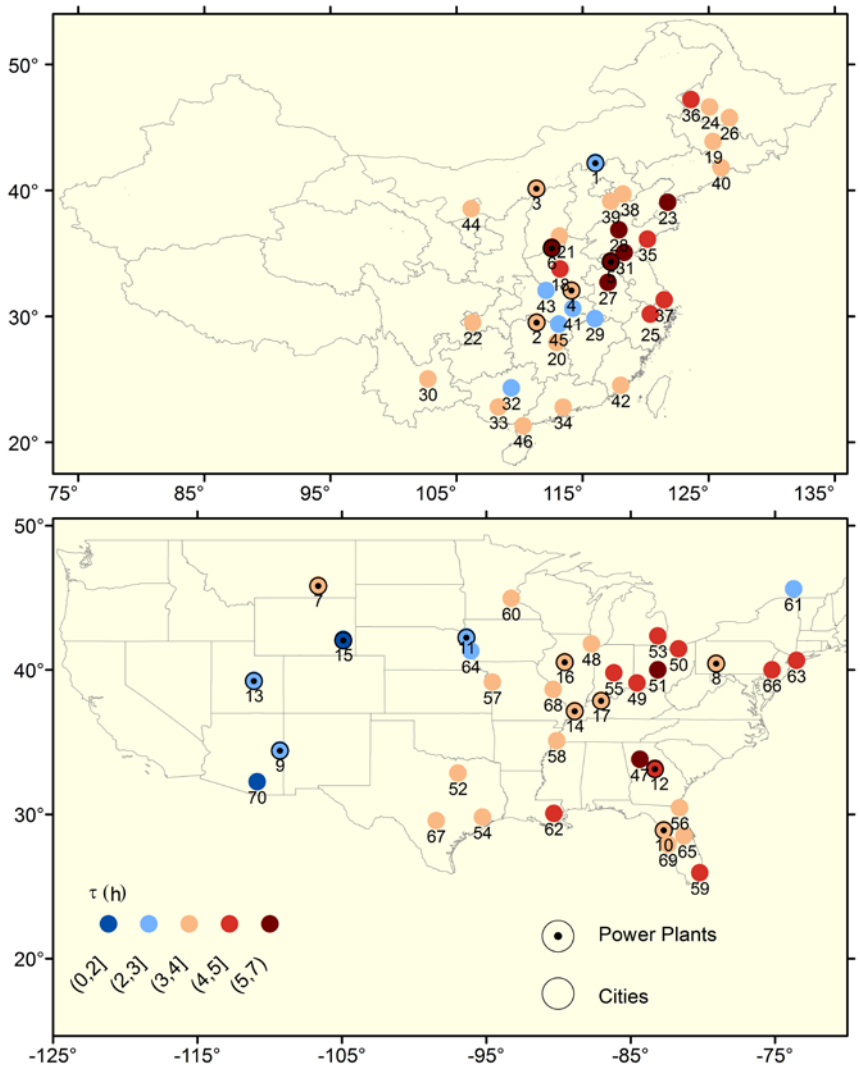


Figure 6. Fitted $NO_x$ lifetimes (color coded) for investigated emission sources over China and the US. Locations of power plants are indicated by dots. Power plants and cities are labelled by their IDs (see Table S2).

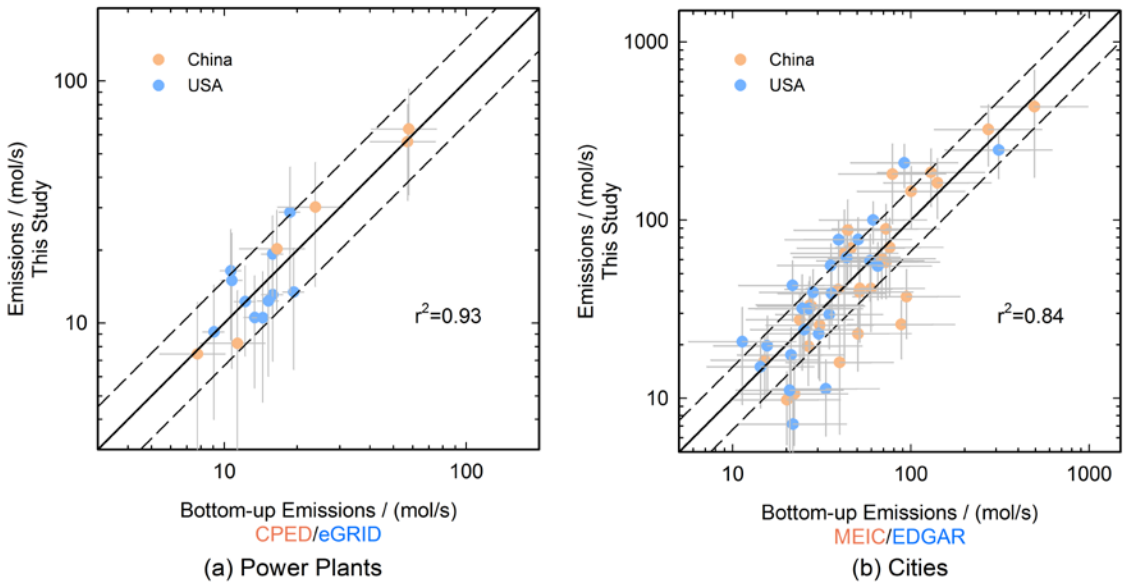


Figure 7. Scatterplots of the derived $NO_x$ emissions for investigated (a) power plants and (b) cities versus bottom-up emission inventories. Emissions are given in mol/s calculated assuming a constant emission rate. Urban emissions from bottom-up inventories are integrated over 40 km ×40 km (see text). Error bars show the uncertainties for emissions by this method (see sect. 2.3) and bottom-up inventories (see sect. 2.4). The straight and dashed lines represent the ratio of 1:1 and 1.5:1/1:1.5, respectively.

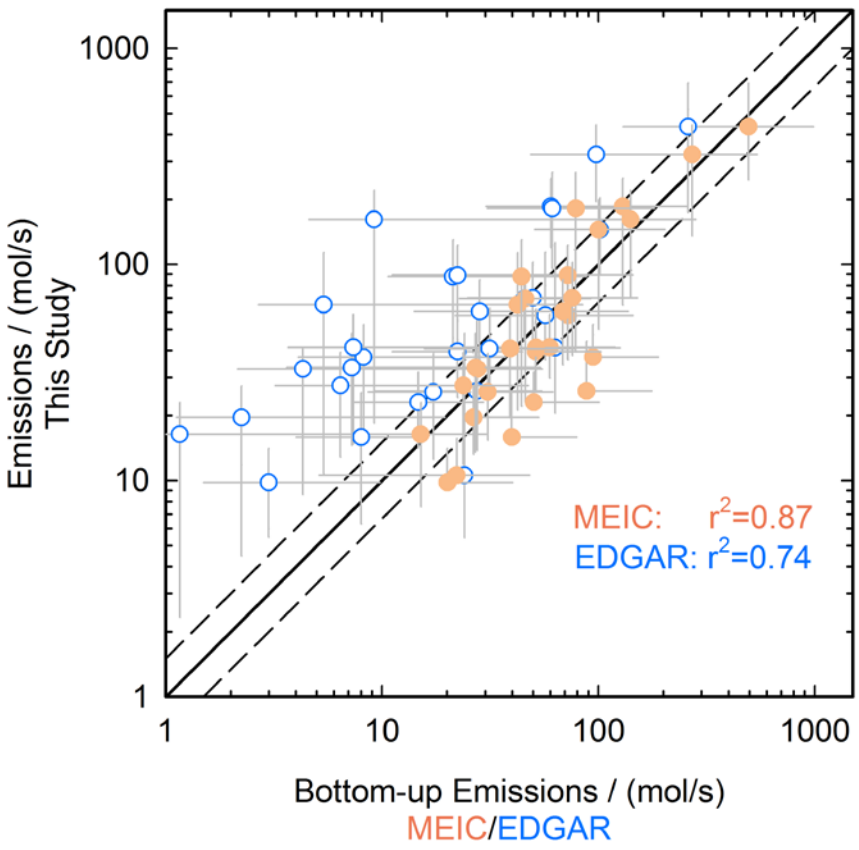


Figure 8. Same as Figure 7 but Scatterplots of the derived $NO_x$ emissions for investigated cities versus MEIC and EDGAR estimates over China.

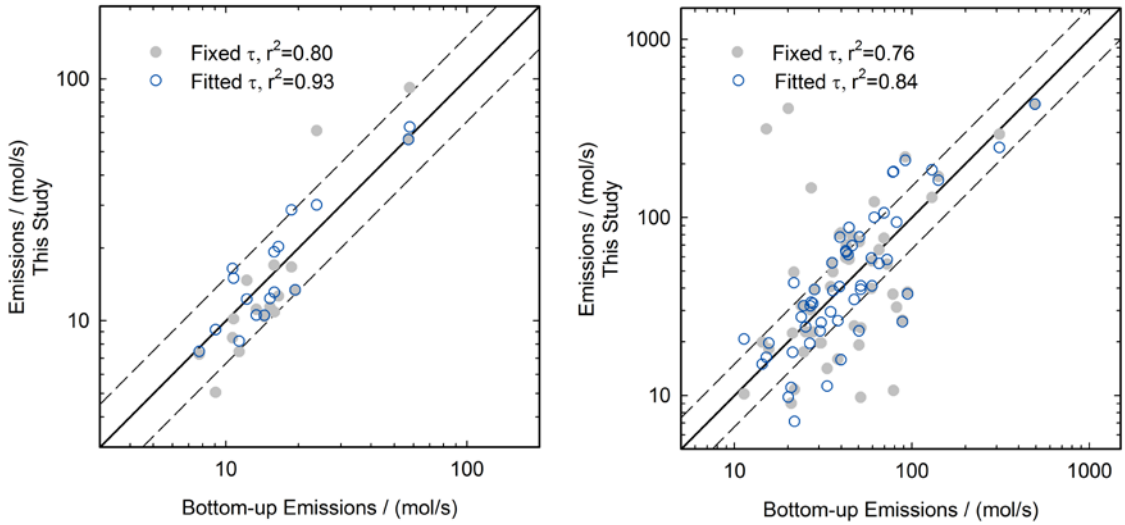


Figure 9. Scatterplots of the resulting $NO_x$ emissions for the investigated power plants and cities using fitted lifetimes (open circles) and fixed lifetimes (3.7 hours) (filled circles) versus the respective estimates from bottom-up emission inventories. Emissions are given in molec/s calculated assuming a constant emission rate. The straight and dashed lines represent the ratio of 1:1 and 1.5:1/1:1.5 respectively.